
VLA-GSE: Boosting Parameter-Efficient Fine-Tuning in VLA with Generalized and Specialized Experts

Yuhua Jiang^{1,2}, Junjie Lu¹, Xinyao Qin^{1,2}, Xiaoyu Chen^{1,2}, Kaixin Wang¹,
Feifei Gao², Li Zhao¹

¹Microsoft Research Asia ²Tsinghua University

Abstract

Vision-language-action (VLA) models inherit rich visual-semantic priors from pre-trained vision-language backbones, but adapting them to robotic control remains challenging. Full fine-tuning (FFT) is prone to overfitting on downstream robotic data and catastrophic forgetting of pretrained vision-language capabilities. Parameter-efficient fine-tuning (PEFT) better preserves pre-trained knowledge, yet existing PEFT methods still struggle to adapt effectively to robot control tasks. To address this gap, we propose **VLA-GSE**, a parameter-efficient VLA fine-tuning framework that improves control adaptation while retaining PEFT’s knowledge preservation advantage. Specifically, VLA-GSE (Generalized and Specialized Experts) is initialized by spectrally decomposing the frozen backbone, assigning leading singular components to generalized experts (shared experts) and disjoint residual components to specialized experts (routed experts). This decomposition improves adaptation capacity under a fixed trainable-parameter budget. Across comparable-budget comparison, VLA-GSE updates only 2.51% of full model parameters and consistently outperforms strong FFT and PEFT baselines. It achieves 81.2% average zero-shot success on LIBERO-Plus, preserves pre-trained VLM capability comparably to LoRA on multimodal understanding benchmarks, and improves real-world manipulation success under multiple distribution shifts. Code is available at <https://github.com/YuhuaJiang2002/VLA-GSE>.

1 Introduction

Vision-language-action (VLA) models have emerged as a compelling paradigm for general-purpose robotic control, where pre-trained vision-language models (VLMs) are adapted into embodied policies [Firoozi et al., 2025, Ma et al., 2024, Zitkovich et al., 2023, Kim et al., 2025b, Zhang et al., 2026, Wu et al., 2026, Chen et al., 2025]. By inheriting strong multimodal priors from foundation VLMs [Dai et al., 2023], these models map visual observations and language instructions to low-level actions, enabling substantial progress in long-horizon manipulation and boarder generalization [Gao et al., 2025, Chen et al., 2024a, Li et al., 2024b, Mees et al., 2022, Ahn et al., 2023, Huang et al., 2025, Shridhar et al., 2023, Black et al., 2024, Jiang et al., 2025, Chen et al., 2024b].

Despite this progress, robust VLM-to-VLA adaptation remains fundamentally challenging. Full fine-tuning (FFT) offers high expressivity but often overfits limited robotic data and degrades pre-trained vision-language competence through catastrophic forgetting [Yang et al., 2026, Li et al., 2024a, Wen et al., 2025, Hancock et al., 2025, Dey et al., 2024, Yang et al., 2025, Yu et al., 2026]. Parameter-efficient fine-tuning (PEFT), such as low-rank adaptation (LoRA), is more stable in preserving pre-trained capability [Hancock et al., 2025], yet existing PEFT approaches frequently under-adapt when precise control is required. This raises a central question: *can PEFT be made sufficiently expressive for precise robot-control adaptation while retaining its knowledge-preservation advantage?*

To address this question, we propose **VLA-GSE (Generalized and Specialized Experts)**, a parameter-efficient VLA fine-tuning framework designed to strengthen adaptation without sacrificing the knowledge retention behavior of PEFT. VLA-GSE is built from a spectral decomposition of the frozen backbone: leading singular components initialize generalized experts (shared experts), while disjoint residual components initialize specialized experts (routed experts). This decomposition concentrates shared capacity in always-available experts, reduces redundancy in routed adaptation, and enables more flexible expert composition for targeted control behaviors.

This design introduces two optimization issues. First, spectral initialization induces large singular-value imbalance across specialized experts, which leads to uneven update magnitudes and weakly trained experts. We address this with *expert-wise gradient scale balancing*, which compensates for spectral imbalance and harmonizes optimization scales. Second, because routing is input-dependent, the equivalent weight becomes sample-dependent and can drift from the frozen backbone at initialization. We address this with a *backbone weight adjustment* mechanism that preserves the backbone-equivalent weight in expectation.

Empirically, VLA-GSE updates only 2.51% of full model parameters yet consistently outperforms strong baselines under a comparable trainable-parameter budget. On LIBERO-Plus, it achieves 81.2% average zero-shot success, exceeding FFT by 6.3% and the strongest PEFT baseline by 4.4%, with strong robustness under diverse perturbations. On multimodal understanding benchmarks, VLA-GSE preserves pre-trained VLM capability comparably to LoRA and outperforms both FFT and co-trained VLA baselines. In real-world evaluation across four manipulation tasks under four distribution shifts, VLA-GSE reaches 82.5% success, outperforming FFT by 16.7%.

2 Related Work and Background

Finetuning VLMs into VLAs. Recent VLA models adapt pre-trained VLMs into robot policies by retaining the multimodal backbone and training additional action modules on robot trajectories [Zhang et al., 2026, Wu et al., 2026, Gao et al., 2025]. Some recent architectures, such as OpenVLA-OFT-style designs, further improve inference efficiency via parallel decoding. Since FFT methods are memory consuming, LoRA is explored in VLA fine-tuning works [Kim et al., 2025b, Hancock et al., 2025, Omaisán and Mohamed, 2025]. In particular, OpenVLA [Kim et al., 2025b] is among the earliest VLA works to adopt LoRA in VLA fine-tuning for lower training memory consumption. VLM2VLA [Hancock et al., 2025] provides evidence that LoRA better preserves pre-trained VLM knowledge during VLA adaptation. Although LoRA-based methods better preserve pre-trained vision-language knowledge than FFT, they often lack sufficient adaptation capacity for precise embodied control. Our method explicitly targets both goals: preserving pretrained multimodal knowledge while enabling stronger downstream control adaptation.

Parameter-Efficient Fine-Tuning. PEFT has become a practical alternative to FFT mainly in LLM finetuning, with LoRA as the canonical example [Hu et al., 2022]. Recent work shows that adapter structure and initialization critically affect adaptation quality: SVD-based methods such as PiSSA, MiLoRA, KaSA, and GOAT exploit different spectral components to better preserve pretrained knowledge or expose task-relevant subspaces [Meng et al., 2024, Wang et al., 2024b,a, Fan et al., 2025], while MoE-style methods such as MoLoRA, AdaMoLE, and HydraLoRA improve capacity through routed low-rank experts [Zadouri et al., 2024, Liu and Luo, 2024, Tian et al., 2024]. However, existing PEFT-based VLA finetuning methods are still largely limited to LoRA-style adaptation [Hancock et al., 2025, Omaisán and Mohamed, 2025], and PEFT remains under-explored in VLA finetuning, where VLA models require stronger adaptation for precise embodied control. Motivated by this difference, VLA-GSE is tailored to the control setting, combining a shared generalized expert with routed specialized experts to support both transferable adaptation and input-specific control refinement. We further introduce gradient scale balancing to stabilize optimization across experts initialized from different spectral components.

3 Method

Overview. Our model follows a standard VLM-to-VLA pipeline, where a pre-trained VLM encodes image observations and language instructions, and an OpenVLA-OFT-style action head is used to generate robot actions [Kim et al., 2025a]. The action head is fully fine-tuned for control and we

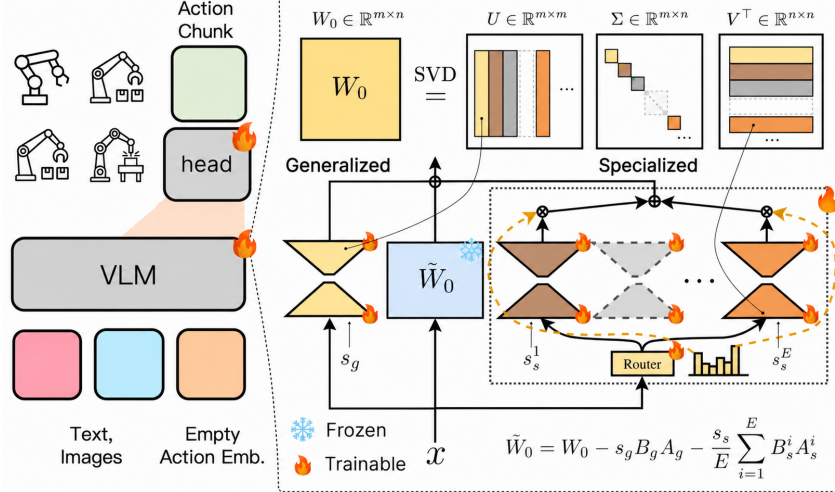


Figure 1: **Overview of the VLA-GSE framework.** (Top Right) VLA-GSE uses an SVD-based adaptive priors scheme to initialize generalized experts and multiple specialized experts based on sorted singular value segments. (Bottom Right) During the forward pass, the output is formed by summing the input transformations induced by the adjusted frozen pre-trained weight \tilde{W}_0 , the generalized expert, and the dynamically selected top- k specialized experts. Unlike prior MoE LoRA, the generalized expert is always active and initialized from the SVD-based priors. GSE is only applied for the pretrained weight W_0 in the VLM.

apply PEFT only to the VLM backbone: for a pre-trained weight $W_0 \in \mathbb{R}^{m \times n}$, we learn a structured low-rank update while keeping most backbone parameters frozen. On top of this foundation, we propose VLA-GSE, which decomposes backbone adaptation into an always-on generalized expert and multiple routed specialized experts. The design is tailored to VLA finetuning, where the model must both preserve pretrained vision-language knowledge and support precise robot control adaptation. VLA-GSE addresses this through generalized-specialized decomposition, expert-wise gradient scale balancing, and backbone weight adjustment.

3.1 Generalized and Specialized Expert Initialization via SVD

We initialize VLA-GSE from the SVD of the frozen pre-trained weight matrix $W_0 \in \mathbb{R}^{m \times n}$: $W_0 = U \Sigma V^T$. Sorting singular values in descending order induces a spectral decomposition of W_0 , from which we allocate the leading components to the *generalized expert* and the *specialized experts*, as illustrated in Figure 1.

Generalized Expert. We allocate the largest r_g singular values to the generalized expert. This expert is tasked with capturing common knowledge and mitigating redundancy in routed experts. Its initialization is formulated as follows:

$$B_g = \sqrt{\frac{1}{s_g}} U_{1:r_g} \Sigma_{1:r_g}^{1/2} \in \mathbb{R}^{m \times r_g}, \quad A_g = \sqrt{\frac{1}{s_g}} \Sigma_{1:r_g}^{1/2} (V_{1:r_g})^T \in \mathbb{R}^{r_g \times n}, \quad W_g = s_g B_g A_g, \quad (1)$$

where $U_{1:r_g}$, $\Sigma_{1:r_g}$, and $V_{1:r_g}$ correspond to the top segment of the SVD, s_g is the scaling factor for the generalized expert, and \tilde{W}_g is the generalized expert’s effective weight. This design is motivated by the observation that leading singular components capture the dominant energy of the pre-trained weight matrix, which makes the always-on adaptation more effective [Meng et al., 2024].

Specialized Experts. The remaining dominant singular components are evenly partitioned to initialize E specialized experts. Under the adaptive prior strategy, we consider the SVD components indexed by $[r_g + 1, r_g + dE]$ and assign each expert a contiguous block of rank d . Formally, let $\mathcal{I}_i \triangleq \{r_g + (i - 1)d + 1, \dots, r_g + id\}, i \in \{1, 2, \dots, E\}$. The i -th specialized expert is then initialized by $U_i = U_{:, \mathcal{I}_i}, \Sigma_i = \Sigma_{\mathcal{I}_i, \mathcal{I}_i}, V_i^T = V_{\mathcal{I}_i, :}^T$. Using these designated segments, the

initialization is formulated as:

$$B_s^i = \sqrt{\frac{1}{s_s^i}} U_i \Sigma_i^{1/2} \in \mathbb{R}^{m \times d}, \quad A_s^i = \sqrt{\frac{1}{s_s^i}} \Sigma_i^{1/2} V_i^\top \in \mathbb{R}^{d \times n}, \quad W_s^i = s_s^i B_s^i A_s^i, \quad (2)$$

where s_s^i is the i -th expert’s scaling factor that normalizes each expert’s scale based on the spectral magnitude of its assigned segment, and W_s^i is the effective weight of the i -th specialized expert.

Specialized Expert Selection Method During the forward pass, a router $W_z \in \mathbb{R}^{E \times n}$ maps the input x to routing logits $z(x)$, which determine a sparse subset of specialized experts for x : $p^i(x) = \frac{\exp(z^i(x))}{\sum_{j=1}^E \exp(z^j(x))}$, $z(x) = W_z x$. Let $\Omega_k(x)$ denote the indices of the top- k $p^i(x)$. The routing weights $w^i(x)$ are explicitly defined by applying a softmax function exclusively over the selected top- k logits:

$$w^i(x) = \begin{cases} \frac{\exp(z^i(x))}{\sum_{j \in \Omega_k(x)} \exp(z^j(x))}, & \text{if } i \in \Omega_k(x), \\ 0, & \text{otherwise.} \end{cases} \quad (3)$$

Load Balancing Auxiliary Loss To prevent the sparse router over-selecting a small subset of specialized experts, we introduce an auxiliary load-balancing loss to encourage balanced expert utilization across GSE blocks. For the l -th GSE block, let $f_i^{(l)}$ denote the fraction of tokens assigned to expert i , and let $P_i^{(l)}$ denote its average routing probability over the batch. We define

$$\mathcal{L}_{\text{bal}}^{(l)} = E \sum_{i=1}^E f_i^{(l)} P_i^{(l)}, \quad \mathcal{L}_{\text{final}} = \|\hat{a} - a\|_1 + \alpha \sum_{l=1}^L \mathcal{L}_{\text{bal}}^{(l)}. \quad (4)$$

The first term in $\mathcal{L}_{\text{final}}$ is the action regression loss and the second term regularizes expert usage. Detailed explanation of load balancing auxiliary loss is shown in Appendix G

3.2 Gradient Scale Balancing.

To avoid optimization imbalance across specialized experts, we analyze their gradient scales at initialization. Let g_A^i and g_B^i denote the localized gradients of the i -th specialized expert with respect to A_s^i and B_s^i , respectively. To characterize the expected gradient scale, we introduce the left and right second-moment matrices of the gradient: $G_L \triangleq \mathbb{E}[g g^\top]$, $G_R \triangleq \mathbb{E}[g^\top g]$. Here, G_L and G_R describe the second-moment structure of g in the left and right subspaces, respectively. The following theorem gives the exact initialization-time gradient scale for each expert.

Theorem 1 (Expert-wise gradient scale balancing). *Let $w^i(x)$ denote the input-dependent routing coefficient multiplying the contribution of the i -th specialized expert in the aggregated equivalent weight for input x . Under the idealized balanced-routing condition at initialization, define $\rho_w := \mathbb{E}_x[(w^i(x))^2]$, and assume that ρ_w is identical across all specialized experts $i \in \{1, \dots, E\}$. Then, for the i -th specialized expert, the expected squared Frobenius norms of its localized gradients satisfy*

$$\mathbb{E}[\|g_A^i\|_F^2] = \rho_w s_s^i \alpha_i^L, \quad \mathbb{E}[\|g_B^i\|_F^2] = \rho_w s_s^i \alpha_i^R, \quad (5)$$

where

$$\alpha_i^L = \text{Tr}(\Sigma_i U_i^\top G_L U_i), \quad \alpha_i^R = \text{Tr}(\Sigma_i V_i^\top G_R V_i). \quad (6)$$

Therefore, under balanced routing, the optimization scale of expert i is determined jointly by its spectral magnitude Σ_i , the projected second-order gradient energy on its corresponding singular subspaces, and a shared routing second-moment factor ρ_w . Moreover, if there exist constants $\kappa_L, \kappa_R > 0$ such that¹

$$\alpha_i^L = \kappa_L \text{Tr}(\Sigma_i), \quad \alpha_i^R = \kappa_R \text{Tr}(\Sigma_i), \quad \forall i \in \{1, \dots, E\}, \quad (7)$$

then choosing

$$s_s^i = s_{\text{base}} \cdot \frac{C}{\text{Tr}(\Sigma_i)} \quad (8)$$

¹This assumption is automatically satisfied under $G_L = \mathbb{E}[g g^\top] \propto I$ and $G_R = \mathbb{E}[g^\top g] \propto I$, which is the commonly used isotropic gradient variance assumption [used in Theorem 1 of Jastrzebski et al., 2018].

equalizes both $\mathbb{E}[\|g_A^i\|_F^2]$ and $\mathbb{E}[\|g_B^i\|_F^2]$ across all specialized experts, since the additional factor ρ_w is shared by all experts under the balanced-routing assumption. Here s_{base} is a global base scaling hyperparameter and C is a normalization constant, e.g., $C = \frac{1}{E} \sum_{j=1}^E \text{Tr}(\Sigma_j)$.

Theorem 1 shows that the trace-inverse scaling rule in Eq. (8) is justified whenever the projected second-order gradient statistics are approximately uniform across experts, as specified in Eq. (7). The detailed proof is provided in Appendix B.

3.3 Backbone Weight Adjustment

Unlike LoRA-style zero perturbation at initialization, VLA-GSE induces a non-zero low-rank perturbation at initialization, which would otherwise shift the weight away from W_0 before fine-tuning. To preserve the pre-trained backbone as much as possible at initialization, we compensate for the non-zero perturbation introduced by the generalized and specialized experts by adjusting the frozen backbone weight from W_0 to \tilde{W}_0 . Let $W_{eq}(x)$ denote the input-dependent equivalent weight of the GSE block. Then, it follows that

$$y = W_{eq}(x)x, \quad W_{eq}(x) = \tilde{W}_0 + s_g B_g A_g + \sum_{i=1}^E w^i(x) s_s^i B_s^i A_s^i. \quad (9)$$

In principle, one may desire an exact sample-wise equality: $W_{eq}(x) = W_0, \forall x$. However, this is generally impossible because the selection of specialized experts varies with x through $w^i(x)$. Accordingly, we aim to maintain consistency with the pretrained weight *in expectation* under the routing distribution at initialization. At random initialization, the router is symmetric across specialized experts in expectation. Since they also satisfy $\sum_{i=1}^E w^i(x) = 1$, we have $\mathbb{E}_x[w^i(x)] = \frac{1}{E}, \forall i \in \{1, \dots, E\}$. It follows that the expected weight of the specialized experts is

$$\mathbb{E}_x \left[\sum_{i=1}^E w^i(x) s_s^i B_s^i A_s^i \right] = \sum_{i=1}^E \mathbb{E}_x[w^i(x)] s_s^i B_s^i A_s^i = \frac{1}{E} \sum_{i=1}^E s_s^i B_s^i A_s^i. \quad (10)$$

This motivates defining the expected residual shift introduced at initialization:

$$W_{res} = s_g B_g A_g + \frac{1}{E} \sum_{i=1}^E s_s^i B_s^i A_s^i, \quad (11)$$

where W_{res} denotes the total expected offset of the initialized GSE weight relative to the original backbone. We then compensate for this offset by redefining the adjusted frozen weight as

$$\tilde{W}_0 = W_0 - W_{res} = W_0 - s_g B_g A_g - \frac{1}{E} \sum_{i=1}^E s_s^i B_s^i A_s^i. \quad (12)$$

Under the backbone weight adjustment in Eq. 12, $W_{eq}(x)$ is aligned with W_0 in expectation at initialization, where the detailed proof is shown in Appendix C. The full initialization and forward-pass procedure is provided in Appendix E.

4 Simulation Experiments

4.1 Settings

Model Architecture and Initialization. In our experiments, we adopt Qwen3-VL-4B-Instruct as the foundation VLM backbone. To efficiently adapt the VLM into a VLA model, we apply our proposed VLA-GSE framework. Specifically, the low-rank dimension is set to $r = 16$. Each GSE block consists of 8 rank-2 experts in total, which explicitly includes 1 generalized expert to anchor the foundational representations, and 7 specialized experts utilizing a Top-2 gating strategy. Scaling across the architecture, this configuration deploys a total of 356 generalized experts and 2492 specialized experts. The initialization strictly follows the SVD-based approach. For the action head, we use the MLP architecture and parallel decoding method from OpenVLA-OFT [Kim et al., 2025a].

Table 1: LIBERO-Plus benchmark zero-shot performance. Results are shown in success rate (%).

Model	Camera	Robot	Language	Light	Background	Noise	Layout	Total
OpenVLA [Kim et al., 2025b]	0.8	3.5	23.0	8.1	34.8	15.2	28.5	15.6
WorldVLA [Cen et al., 2025]	0.1	27.9	41.6	43.7	17.1	10.9	38.0	25.0
NORA [Hung et al., 2025]	2.2	37.0	65.1	45.7	58.6	12.8	62.1	39.0
UniVLA [Bu et al., 2025]	1.8	46.2	69.6	69.0	81.0	21.2	31.9	42.9
π_0 [Black et al., 2024]	13.8	6.0	58.8	85.0	81.4	79.0	68.9	53.6
π_0 -Fast [Pertsch et al., 2025]	65.1	21.6	61.0	73.2	73.2	74.4	68.8	61.6
OpenVLA-OFT [Kim et al., 2025a]	56.4	31.9	79.5	88.7	93.3	75.8	74.2	69.6
RIPT-VLA [Tan et al., 2025]	55.2	31.2	77.6	88.4	91.6	73.5	74.2	68.4
ABot-M0 [Yang et al., 2026]	60.4	67.9	86.4	96.2	91.6	86.4	82.6	80.5
VLANeXt [Wu et al., 2026]	71.6	63.4	81.4	93.7	91.8	89.5	77.7	80.1
VLA-GSE (Ours)	64.4	68.5	88.8	97.3	97.3	79.4	82.6	81.2

Optimization and Hyperparameters. The model is trained from Qwen3-VL-4B-Instruct for a total of 80,000 optimization steps. The batch size per GPU is set to 16, resulting in an effective total batch size of 128 across 8 NVIDIA A100 GPUs. To ensure stable adaptation while preventing the catastrophic forgetting of pre-trained visual-semantic knowledge, we apply decoupled learning rates: the learning rate for the GSE parameters in VLM is set to 1×10^{-5} , while the newly initialized action MLP head uses a learning rate of 1×10^{-4} . Furthermore, the auxiliary load-balancing loss weight α is set to 0.01. We set the generalized scaling factor as $s_g = 2$ and set the i -th specialized scaling factor as $s_s^i = \frac{2 \sum_{j=1}^E \text{Tr}(\Sigma_j)}{E \cdot \text{Tr}(\Sigma_i)}$. In this way, the scaling of each specialized expert is inversely proportional to its spectral magnitude. A comprehensive summary of the detailed hyperparameter settings and model configurations is provided in Appendix Table 9.

Parameter Efficiency. Training VLA-GSE is highly parameter-efficient. Among the 4,551.85M total model parameters, we freeze 4,437.82M non-GSE parameters from the base VLM and optimize only 114.04M parameters (2.51% of the full model). Specifically, the trainable parameters consist of 48.41M parameters in the GSE modules and 65.62M parameters in the action head.

4.2 LIBERO-Plus Benchmark Results

We use LIBERO-Plus [Fei et al., 2025] as the simulation benchmark, which evaluates VLA models’ generalization ability across seven perturbation dimensions. All models are trained using the combined training sets from all 4 suites of LIBERO [Liu et al., 2023]. Table 1 shows that VLA-GSE achieves the best overall zero-shot performance, obtaining 81.2% average success and outperforming the strongest prior baselines, including ABot-M0 (80.5%) and VLANeXt (80.1%). The improvement is broad rather than isolated: VLA-GSE delivers the strongest average robustness on Robot, Language, Light, and Background, while matching the best Layout performance. At the suite level, it attains 90.3% on Spatial and 86.2% on Object, and remains stable on the more challenging Goal and Long suites with 74.2% and 74.1%, respectively. Overall, these results indicate that VLA-GSE improves not only aggregate success rate, but also robustness under diverse test-time perturbations. The full suite-wise results of VLA-GSE are provided in Appendix D.5.

Table 2 compares fine-tuning strategies in LIBERO-Plus zero-shot generalization using the Qwen3-VL-4B-Instruct backbone. For a fair comparison, all PEFT methods use roughly 2.51% (114M) trainable parameters and are independently tuned for optimal performance. Notably, FFT (74.9%) underperforms several PEFT baselines due to *catastrophic forgetting* [Hancock et al., 2025, Yu et al., 2026], where updating all parameters overwrites the backbone’s generalized priors and degrades zero-shot capabilities. Our method, VLA-GSE, successfully mitigates this by balancing knowledge retention with efficient adaptation, achieving the highest overall success rate of 81.2%. It outperforms FFT by 6.3 points and the strongest baseline, GOAT, by 4.4 points on average in all seven zero-shot dimensions. These results demonstrate that VLA-GSE is significantly more robust and effective for VLA fine-tuning than conventional LoRA-style, SVD-based, or LoRA-MoE variants.

We qualitatively illustrate the attention maps in the challenging **dark lighting** setting of LIBERO-Plus. Figure 2 shows the last transformer layer attention maps for different models under the instruction: “Pick up the black bowl between the plate and the ramekin and place it on the plate.” Both FFT and LoRA are fine-tuned from the same Qwen3-VL-4B-Instruct backbone. VLA-GSE exhibits concentrated attention on the **graspable edges** of the correct target object and successfully completes

Table 2: Finetuning method comparison based on LIBERO-Plus benchmark zero-shot performance. Results are shown in success rate (%).

Model	Params (%)	Camera	Robot	Language	Light	Background	Noise	Layout	Total
FFT (Full Fine-Tuning)	100.00	45.8	60.5	86.9	95.9	94.7	74.1	79.2	74.9
LoRA [Hu et al., 2022]	2.58	44.3	53.6	82.1	92.9	91.1	67.1	67.2	69.2
rsLoRA [Kalajdziewski, 2023]	2.52	46.0	58.9	85.1	93.6	92.4	71.6	76.5	73.1
DoRA [Liu et al., 2024]	2.54	49.7	61.0	86.6	95.7	94.4	73.4	78.6	75.3
PiSSA [Meng et al., 2024]	2.54	48.3	59.4	86.0	95.4	94.0	72.8	78.1	74.5
MoLoRA [Zadouri et al., 2024]	2.56	52.2	61.5	87.5	96.0	95.0	74.2	79.0	76.2
AdaMoLE [Liu and Luo, 2024]	2.53	50.2	60.8	87.8	95.8	94.4	73.1	78.6	75.5
HydraLoRA [Tian et al., 2024]	2.55	51.3	60.1	86.4	95.4	94.1	73.0	78.2	75.2
MiLoRA [Wang et al., 2025]	2.52	51.1	60.1	86.3	94.9	93.9	73.0	77.7	75.0
GOAT [Fan et al., 2025]	2.54	54.5	61.8	87.7	96.2	95.2	74.6	79.3	76.8
VLA-GSE (Ours)	2.51	64.4	68.5	88.8	97.3	97.3	79.4	82.6	81.2



Figure 2: Attention map visualizations for different models under the LIBERO-Plus **dark lighting** environment. The instruction is “Pick up the black bowl between the plate and the ramekin and place it on the plate.” Our VLA-GSE method exhibits precise attention on the **graspable edges** of the target object, whereas π_0 , $\pi_{0.5}$, FFT, and LoRA show scattered attention or focus on incorrect objects.

the task, indicating that it not only identifies the target specified by the dense spatial instruction, but also captures the manipulation affordance required for grasping, namely the appropriate edge positions for the gripper. In contrast, the baselines show either scattered or mislocalized attention, leading to incorrect object selection or failed grasping. These results suggest that GSE better preserves the backbone’s visual-semantic grounding while acquiring task-specific manipulation behavior. More qualitative examples are provided in Figure 4.

4.3 Knowledge Retention after VLA Fine-Tuning in Terms of Multimodal Understanding

We further evaluate the base VLM and VLA-adapted variants on a diverse set of multimodal understanding benchmarks. As shown in Table 3, FFT leads to a clear and consistent degradation across benchmarks, indicating severe catastrophic forgetting of pretrained vision–language capability during VLM-to-VLA transfer. A similar trend is also observed for co-trained VLA models such as $\pi_{0.5}$, whose multimodal understanding performance remains far from that of strong general-purpose VLMs, suggesting that preserving VLM knowledge is still challenging under FFT embodied training.

In contrast, both Qwen3-VL-LoRA and VLA-GSE remain consistently close to the base Qwen3-VL-4B-Instruct on general multimodal benchmarks, showing substantially better preservation of pretrained multimodal knowledge than FFT. Importantly, VLA-GSE achieves a retention level comparable to standard LoRA-based PEFT, which suggests that its stronger embodied performance does not come from sacrificing the original vision–language capability. Instead, VLA-GSE preserves pretrained VLM knowledge similarly well to LoRA, while providing stronger adaptation capacity for downstream robotic control as shown in Table 2.

4.4 Ablation Study

To isolate the contributions of our core designs, we conduct an ablation study on the LIBERO-Plus zero-shot Long suite. The “w.o. SVD Initialization” variant instead uses a standard LoRA-style initialization, with each B_s^i Gaussian initialized and each A_s^i zero initialized. For the expert routing ablations, we maintain a constant total number of experts to ensure a fair comparison of model

Table 3: Multimodal understanding evaluation. Comparison of VLMs and VLAs across multimodal understanding benchmarks.

Method	#Params	MMMU	MMStar	OCRBench	MMB-en	DocVQA	InfoVQA	AI2D	RealWorldQA
Prismatic VLM Family									
Prismatic VLM [Karamcheti et al., 2024]	7B	35.0	38.8	32.0	66.2	17.5	19.7	54.6	30.8
OpenVLA [Kim et al., 2025b]	7B	26.3	0	0	0	0	0	0	0
ECot [Zawalski et al., 2025]	7B	26.6	0	0.01	3.7	0	0	0	25.6
Gemma-3 Family									
Gemma-3-4B-IT [Gemma Team, 2025]	4B	39.3	37.1	70.2	68.6	68.8	40.9	70.5	44.0
Gemma-3-12B-IT [Gemma Team, 2025]	12B	46.0	46.3	75.0	76.9	80.6	50.4	78.5	50.6
VLM2VLA-AT [Hancock et al., 2025]	12B	45.9	45.2	65.5	70.9	74.6	44.8	74.1	44.5
VLM2VLA [Hancock et al., 2025]	12B	42.7	48.0	63.9	68.5	78.4	46.2	74.0	43.3
Other Baseline VLAs									
MolmoAct [Lee et al., 2025]	7B	28.4	1.2	52.7	55.1	58.7	41.9	2.0	8.6
$\pi_{0.5}$ [Black et al., 2025a]	3B	24.0	21.7	6.8	6.8	4.6	7.7	27.0	2.7
Qwen3-VL Family									
Qwen3-VL-4B-Instruct [Bai et al., 2025]	4B	53.2	69.8	88.1	85.1	95.3	80.3	84.1	70.9
Qwen3-VL-FFT [Bai et al., 2025]	4B	35.6	31.4	43.2	50.8	55.1	37.6	48.3	33.7
Qwen3-VL-LoRA [Bai et al., 2025]	4B	51.8	68.1	83.3	83.0	94.1	79.2	83.0	69.8
VLA-GSE (Ours)	4B	51.1	67.8	85.6	82.4	92.8	78.5	83.4	70.1

Table 4: Ablation study on Long suite of LIBERO-Plus benchmark zero-shot performance. Results are shown in success rate (%).

Model	Camera	Robot	Language	Light	Background	Noise	Layout	Total
w.o. SVD Initialization	25.8	41.9	80.8	84.8	88.1	51.0	70.3	60.9
w.o. Generalized Experts	25.1	50.2	84.4	95.7	85.9	62.5	81.9	67.2
w.o. Specialized Experts	24.0	48.8	82.8	88.7	90.6	52.1	71.4	63.1
w.o. Auxiliary Loss	32.2	59.7	90.0	91.8	96.8	62.9	85.4	72.0
w.o. Gradient Scaling	32.5	59.5	90.2	91.6	96.5	63.1	85.6	72.1
VLA-GSE (Ours)	35.8	61.0	91.0	94.9	98.3	65.2	87.3	74.1

capacity. Specifically, the “w.o. Generalized Experts” setting replaces the generalized expert with an additional specialized expert, forcing the model to rely entirely on routing mechanisms. Conversely, the “w.o. Specialized Experts” variant replaces all specialized experts with generalized ones. The “w.o. Auxiliary Loss” variant removes the load-balancing objective during training. Finally, the “w.o. Gradient Scaling” variant replaces the expert-wise trace-inverse scaling in Eq. 8 with a constant scaling factor, setting all s_s^i to 2.

Our full GSE framework achieves the highest overall success rate of 74.1%, significantly outperforming all ablated variants. The most severe degradation occurs without SVD initialization. Replacing either expert type also causes notable drops, showing that merely increasing parameter capacity is insufficient: the generalized expert provides robust visual-semantic grounding and mitigates overfitting, while the specialized experts decouple complex manipulation strategies under high-variance conditions such as Noise and Layout. Removing the auxiliary loss reduces the overall success rate to 72.0%, demonstrating that unconstrained routing can lead to expert collapse and suboptimal module utilization. The “w.o. Gradient Scaling” variant yields a comparable result of 72.1%, suggesting that the proposed scaling initialization in Theorem 1 is also important for balancing expert-wise optimization dynamics; without it, uneven gradient magnitudes can cause certain experts to dominate training while others remain under-optimized.

5 Real-World Experiments

To further validate our framework, we conduct extensive real-world experiments on the AgileX PiPER robot. The robot is equipped with a fixed front-view camera and a wrist camera for visual observation. As illustrated in Figure 3, the real-world benchmark consists of four tasks: *Pour water into bowl*, *Pick spoon into plate*, *Put carrot into bowl*, and *Take pen out of pen container*. Each task is further evaluated under four types of distribution shifts: lighting changes, language variations, cluttered layout variations, and background tablecloth changes. For each generalization dimension, we collect 15 test cases, resulting in 60 trials per task.

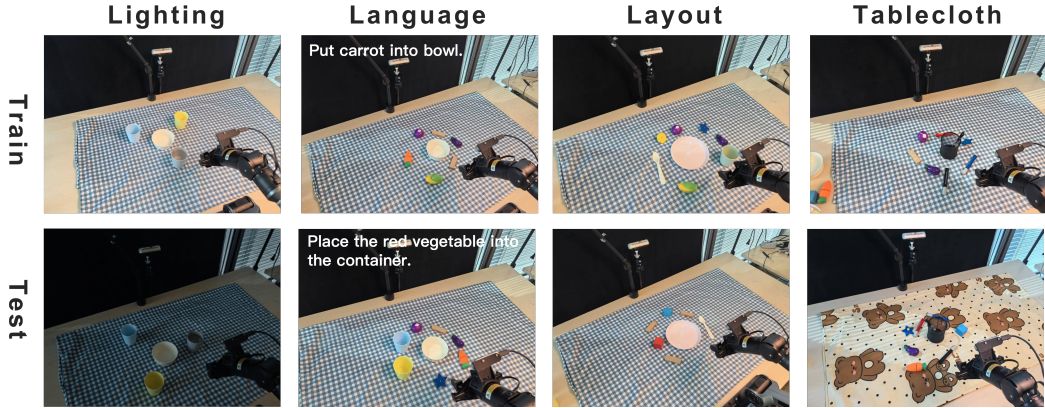


Figure 3: **Real-world generalization settings.** The four train-test pairs correspond to variations in *lighting*, *language*, *clutter layout*, and *background tablecloth*, respectively. For *language* variations, the training instruction is “Put carrot into bowl.” At test time, we replace it with “Place the red vegetable into the container.”

Table 5: Results on **real-world** generalization. Each task contains 60 evaluation episodes, including 4 OOD settings: variations in *lighting*, *language*, *clutter layout*, and *background tablecloth*. Results are reported in success rate (%).

Model	Pour water into bowl	Pick spoon into plate	Put carrot into bowl	Take pen out of pen container	Average
OpenVLA-OFT [Kim et al., 2025a]	38.3	41.7	48.3	43.3	42.9
π_0 [Black et al., 2024]	51.7	55.0	60.0	56.7	55.8
$\pi_{0.5}$ [Black et al., 2025a]	73.3	76.7	75.0	71.7	74.2
Qwen3-VL-LoRA [StarVLA, 2026]	58.3	61.7	66.7	60.0	61.7
Qwen3-VL-FFT [StarVLA, 2026]	63.3	66.7	70.0	63.3	65.8
VLA-GSE (Ours)	81.7	85.0	83.3	80.0	82.5

Table 5 summarizes the real-world generalization results. VLA-GSE achieves the best performance on all 4 tasks, yielding the highest average success rate of 82.5%. Among the baselines, $\pi_{0.5}$ is the strongest, followed by Qwen3-VL-FFT, Qwen3-VL-LoRA, and π_0 , while OpenVLA-OFT performs the worst. Notably, Qwen3-VL-LoRA consistently underperforms Qwen3-VL-FFT across all tasks, which aligns with the trend observed in Table 2: parameter-efficient adaptation improves transferability, but FFT remains more effective than vanilla low-rank adaptation for acquiring robust action grounding. By contrast, VLA-GSE delivers a clear margin over all baselines, indicating that its generalized-specialized decomposition is better suited for handling real-world distribution shifts in illumination, background, clutter layout, and instruction phrasing. We also compare real-world inference time between VLA-GSE and baselines in Appendix D.4.

6 Conclusion

We present VLA-GSE, a parameter-efficient framework for adapting pre-trained VLMs to VLA policies that improves control adaptation while retaining the knowledge-preservation benefits of PEFT. VLA-GSE combines a generalized expert (shared adaptation path) with routed specialized experts, together with SVD-based initialization, expert-wise gradient scale balancing, and expectation-based backbone weight adjustment, to increase adaptation capacity for precise robotic control under a fixed trainable-parameter budget. Empirically, VLA-GSE consistently outperforms strong FFT and PEFT baselines on simulation and real-world manipulation benchmarks under a comparable trainable-parameter budget, while preserving pre-trained VLM capability comparably to LoRA and outperforming both FFT and co-trained baseline VLA models. Overall, these results position effective PEFT as a promising direction for VLM-to-VLA adaptation and as a practical, compute-efficient alternative to heavy co-training strategies that require substantial vision-language data for knowledge preservation.

References

- Michael Ahn, Anthony Brohan, Noah Brown, Yevgen Chebotar, Omar Cortes, Byron David, Chelsea Finn, Chuyuan Fu, Keerthana Gopalakrishnan, Karol Hausman, Alex Herzog, Daniel Ho, Jasmine Hsu, Julian Ibarz, Brian Ichter, Alex Irpan, Eric Jang, Rosario Jauregui Ruano, Kyle Jeffrey, Sally Jesmonth, Nikhil J Joshi, Ryan Julian, Dmitry Kalashnikov, Yuheng Kuang, Kuang-Huei Lee, Sergey Levine, Yao Lu, Linda Luu, Carolina Parada, Peter Pastor, Jornell Quiambao, Kanishka Rao, Jarek Rettinghouse, Diego Reyes, Pierre Sermanet, Nicolas Sievers, Clayton Tan, Alexander Toshev, Vincent Vanhoucke, Fei Xia, Ted Xiao, Peng Xu, Sichun Xu, Mengyuan Yan, and Andy Zeng. Do as i can, not as i say: Grounding language in robotic affordances. In *Proceedings of The 7th Conference on Robot Learning*, Proceedings of Machine Learning Research, pages 287–318, 2023.
- Shuai Bai, Yuxuan Cai, Ruizhe Chen, Keqin Chen, Xionghui Chen, Zesen Cheng, Lianghao Deng, Wei Ding, Chang Gao, Chunjiang Ge, Wenbin Ge, Zhifang Guo, Qidong Huang, Jie Huang, Fei Huang, Binyuan Hui, Shutong Jiang, Zhaohai Li, Mingsheng Li, Mei Li, Kaixin Li, Zicheng Lin, Junyang Lin, Xuejing Liu, Jiawei Liu, Chenglong Liu, Yang Liu, Dayiheng Liu, Shixuan Liu, Dunjie Lu, Ruilin Luo, Chenxu Lv, Rui Men, Lingchen Meng, Xuancheng Ren, Xingzhang Ren, Sibao Song, Yuchong Sun, Jun Tang, Jianhong Tu, Jianqiang Wan, Peng Wang, Pengfei Wang, Qiuyue Wang, Yuxuan Wang, Tianbao Xie, Yiheng Xu, Haiyang Xu, Jin Xu, Zhibo Yang, Mingkun Yang, Jianxin Yang, An Yang, Bowen Yu, Fei Zhang, Hang Zhang, Xi Zhang, Bo Zheng, Humen Zhong, Jingren Zhou, Fan Zhou, Jing Zhou, Yuanzhi Zhu, and Ke Zhu. Qwen3-vl technical report. *arXiv preprint arXiv:2511.21631*, 2025. doi: 10.48550/arXiv.2511.21631.
- Kevin Black, Noah Brown, Danny Driess, Adnan Esmail, Michael Equi, Chelsea Finn, Niccolo Fusai, Lachy Groom, Karol Hausman, Brian Ichter, Szymon Jakubczak, Tim Jones, Liyiming Ke, Sergey Levine, Adrian Li-Bell, Mohith Mothukuri, Suraj Nair, Karl Pertsch, Lucy Xiaoyang Shi, James Tanner, Quan Vuong, Anna Walling, Haohuan Wang, and Ury Zhilinsky. π_0 : A vision-language-action flow model for general robot control. *arXiv preprint arXiv:2410.24164*, 2024.
- Kevin Black, Noah Brown, James Darpinian, Karan Dhabalia, Danny Driess, Adnan Esmail, Michael Equi, Chelsea Finn, Niccolo Fusai, Manuel Y. Galliker, Dibya Ghosh, Lachy Groom, Karol Hausman, Brian Ichter, Szymon Jakubczak, Tim Jones, Liyiming Ke, Devin LeBlanc, Sergey Levine, Adrian Li-Bell, Mohith Mothukuri, Suraj Nair, Karl Pertsch, Allen Z. Ren, Lucy Xiaoyang Shi, Laura Smith, Jost Tobias Springenberg, Kyle Stachowicz, James Tanner, Quan Vuong, Homer Walke, Anna Walling, Haohuan Wang, Lili Yu, and Ury Zhilinsky. $\pi_{0.5}$: a vision-language-action model with open-world generalization, 2025a. URL <https://arxiv.org/abs/2504.16054>.
- Kevin Black, Noah Brown, Danny Driess, Adnan Esmail, Michael Robert Equi, Chelsea Finn, Niccolo Fusai, Lachy Groom, Karol Hausman, Brian Ichter, Szymon Jakubczak, Tim Jones, Liyiming Ke, Sergey Levine, Adrian Li-Bell, Mohith Mothukuri, Suraj Nair, Karl Pertsch, Lucy Xiaoyang Shi, Laura Smith, James Tanner, Quan Vuong, Anna Walling, Haohuan Wang, and Ury Zhilinsky. π_0 : A Vision-Language-Action Flow Model for General Robot Control. In *Proceedings of Robotics: Science and Systems*, Los Angeles, CA, USA, June 2025b. doi: 10.15607/RSS.2025.XXI.010.
- Qingwen Bu, Yanting Yang, Jisong Cai, Shenyuan Gao, Guanghui Ren, Maoqing Yao, Ping Luo, and Hongyang Li. UniVLA: Learning to act anywhere with task-centric latent actions, 2025. URL <https://arxiv.org/abs/2505.06111>.
- Jun Cen, Chaohui Yu, Hangjie Yuan, Yuming Jiang, Siteng Huang, Jiayan Guo, Xin Li, Yibing Song, Hao Luo, Fan Wang, Deli Zhao, and Hao Chen. WorldVLA: Towards autoregressive action world model, 2025. URL <https://arxiv.org/abs/2506.21539>.
- Boyuan Chen, Zhuo Xu, Sean Kirmani, Brian Ichter, Danny Driess, Pete Florence, Dorsa Sadigh, Leonidas Guibas, and Fei Xia. SpatialVLM: Endowing vision-language models with spatial reasoning capabilities. In *Proceedings of the IEEE/CVF Conference on Computer Vision and Pattern Recognition*, pages 14455–14465, 2024a.
- Xiaoyu Chen, Junliang Guo, Tianyu He, Chuheng Zhang, Pushi Zhang, Derek Cathera Yang, Li Zhao, and Jiang Bian. Igor: Image-goal representations are the atomic control units for foundation models in embodied ai. *arXiv preprint arXiv:2411.00785*, 2024b.
- Xiaoyu Chen, Hangxing Wei, Pushi Zhang, Chuheng Zhang, Kaixin Wang, Yanjiang Guo, Rushuai Yang, Yucen Wang, Xinquan Xiao, Li Zhao, et al. Villa-x: enhancing latent action modeling in vision-language-action models. *arXiv preprint arXiv:2507.23682*, 2025.
- Cheng Chi, Siyuan Feng, Yilun Du, Zhenjia Xu, Eric Cousineau, Benjamin CM Burchfiel, and Shuran Song. Diffusion Policy: Visuomotor Policy Learning via Action Diffusion. In *Proceedings of Robotics: Science and Systems*, Daegu, Republic of Korea, July 2023. doi: 10.15607/RSS.2023.XIX.026.

- StarVLA Community. Starvla: A lego-like codebase for vision-language-action model developing, 2026. URL <https://arxiv.org/abs/2604.05014>.
- Damai Dai, Chengqi Deng, Chenggang Zhao, R. X. Xu, Huazuo Gao, Deli Chen, Jiashi Li, Wangding Zeng, Xingkai Yu, Y. Wu, Zhenda Xie, Y. K. Li, Panpan Huang, Fuli Luo, Chong Ruan, Zhifang Sui, and Wenfeng Liang. Deepseekmoe: Towards ultimate expert specialization in mixture-of-experts language models. *arXiv preprint arXiv:2401.06066*, 2024.
- Wenliang Dai, Junnan Li, Dongxu Li, Anthony Meng Huat Tiong, Junqi Zhao, Weisheng Wang, Boyang Li, Pascale Fung, and Steven Hoi. Instructblip: Towards general-purpose vision-language models with instruction tuning. In *Advances in Neural Information Processing Systems*, volume 36, 2023.
- Sombit Dey, Jan-Nico Zaech, Nikolay Nikolov, Luc Van Gool, and Danda Pani Paudel. Revla: Reverting visual domain limitation of robotic foundation models. *arXiv preprint arXiv:2409.15250*, 2024.
- Chenghao Fan, Zhenyi Lu, Sichen Liu, Xiaoye Qu, Wei Wei, Chengfeng Gu, and Yu Cheng. Make lora great again: Boosting lora with adaptive singular values and mixture-of-experts optimization alignment. In *Proceedings of the 42nd International Conference on Machine Learning*, 2025.
- William Fedus, Barret Zoph, and Noam Shazeer. Switch transformers: Scaling to trillion parameter models with simple and efficient sparsity. *Journal of Machine Learning Research*, 23(120):1–39, 2022.
- Senyu Fei, Siyin Wang, Junhao Shi, Zihao Dai, Jikun Cai, Pengfang Qian, Li Ji, Xinzhe He, Shiduo Zhang, Zhaoye Fei, Jinlan Fu, Jingjing Gong, and Xipeng Qiu. Libero-plus: In-depth robustness analysis of vision-language-action models. *arXiv preprint arXiv:2510.13626*, 2025.
- Roya Firoozi, Johnathan Tucker, Stephen Tian, Anirudha Majumdar, Jiankai Sun, Weiyu Liu, Yuke Zhu, Shuran Song, Ashish Kapoor, Karol Hausman, Brian Ichter, Danny Driess, Jiajun Wu, Cewu Lu, and Mac Schwager. Foundation models in robotics: Applications, challenges, and the future. *The International Journal of Robotics Research*, 44(5), 2025. doi: 10.1177/02783649241281508.
- Chongkai Gao, Zixuan Liu, Zhenghao Chi, Junshan Huang, Xin Fei, Yiwen Hou, Yuxuan Zhang, Yudi Lin, Zhirui Fang, Zeyu Jiang, and Lin Shao. Vla-os: Structuring and dissecting planning representations and paradigms in vision-language-action models. *arXiv preprint arXiv:2506.17561*, 2025.
- Gemma Team. Gemma 3 technical report. *arXiv preprint arXiv:2503.19786*, 2025. doi: 10.48550/arXiv.2503.19786.
- Asher J. Hancock, Xindi Wu, Lihan Zha, Olga Russakovsky, and Anirudha Majumdar. Actions as language: Fine-tuning vlms into vlas without catastrophic forgetting. *arXiv preprint arXiv:2509.22195*, 2025.
- Zhi Hou, Tianyi Zhang, Yuwen Xiong, Haonan Duan, Hengjun Pu, Ronglei Tong, Chengyang Zhao, Xizhou Zhu, Yu Qiao, Jifeng Dai, and Yuntao Chen. Dita: Scaling diffusion transformer for generalist vision-language-action policy. In *Proceedings of the IEEE/CVF International Conference on Computer Vision (ICCV)*, pages 7686–7697, October 2025.
- Edward J. Hu, Yelong Shen, Phillip Wallis, Zeyuan Allen-Zhu, Yuanzhi Li, Shean Wang, Lu Wang, and Weizhu Chen. Lora: Low-rank adaptation of large language models. In *International Conference on Learning Representations*, 2022. URL <https://openreview.net/forum?id=nZeVKeeFYf9>.
- Chi-Pin Huang, Yueh-Hua Wu, Min-Hung Chen, Yu-Chiang Frank Wang, and Fu-En Yang. Thinkact: Vision-language-action reasoning via reinforced visual latent planning. *arXiv preprint arXiv:2507.16815*, 2025.
- Chia-Yu Hung, Qi Sun, Pengfei Hong, Amir Zadeh, Chuan Li, U-Xuan Tan, Navonil Majumder, and Soujanya Poria. Nora: A small open-sourced generalist vision language action model for embodied tasks, 2025. URL <https://arxiv.org/abs/2504.19854>.
- Stanisław Jastrzębski, Zachary Kenton, Devansh Arpit, Nicolas Ballas, Asja Fischer, Yoshua Bengio, and Amos Storkey. Three factors influencing minima in sgd. In *International Conference on Learning Representations*, 2018. URL <https://openreview.net/forum?id=rJma2bZCW>.
- Yuhua Jiang, Shuang Cheng, Yan Ding, Feifei Gao, and Biqing Qi. AsyncVLA: Asynchronous flow matching for Vision-Language-Action models, 2025. URL <https://arxiv.org/abs/2511.14148>.
- Damjan Kalajdziewski. A rank stabilization scaling factor for fine-tuning with lora. *arXiv preprint arXiv:2312.03732*, 2023. URL <https://arxiv.org/abs/2312.03732>.

- Siddharth Karamcheti, Suraj Nair, Ashwin Balakrishna, Percy Liang, Thomas Kollar, and Dorsa Sadigh. Prismatic VLMs: Investigating the design space of visually-conditioned language models. In Ruslan Salakhutdinov, Zico Kolter, Katherine Heller, Adrian Weller, Nuria Oliver, Jonathan Scarlett, and Felix Berkenkamp, editors, *Proceedings of the 41st International Conference on Machine Learning*, volume 235 of *Proceedings of Machine Learning Research*, pages 23123–23144. PMLR, 21–27 Jul 2024. URL <https://proceedings.mlr.press/v235/karamcheti24a.html>.
- Moo Jin Kim, Chelsea Finn, and Percy Liang. Fine-tuning vision-language-action models: Optimizing speed and success. *arXiv preprint arXiv:2502.19645*, 2025a.
- Moo Jin Kim, Karl Pertsch, Siddharth Karamcheti, Ted Xiao, Ashwin Balakrishna, Suraj Nair, Rafael Rafailov, Ethan P Foster, Pannag R Sanketi, Quan Vuong, Thomas Kollar, Benjamin Burchfiel, Russ Tedrake, Dorsa Sadigh, Sergey Levine, Percy Liang, and Chelsea Finn. Openvla: An open-source vision-language-action model. In *Proceedings of The 8th Conference on Robot Learning*, volume 270 of *Proceedings of Machine Learning Research*, pages 2679–2713, 2025b.
- Jason Lee, Jiafei Duan, Haoquan Fang, Yuquan Deng, Shuo Liu, Boyang Li, Bohan Fang, Jieyu Zhang, Yi Ru Wang, Sangho Lee, Winson Han, Wilbert Pumacay, Angelica Wu, Rose Hendrix, Karen Farley, Eli VanderBilt, Ali Farhadi, Dieter Fox, and Ranjay Krishna. Molmoact: Action reasoning models that can reason in space. *arXiv preprint arXiv:2508.07917*, 2025. doi: 10.48550/arXiv.2508.07917.
- Wei Li, Renshan Zhang, Rui Shao, Jie He, and Liqiang Nie. Cogvla: Cognition-aligned vision-language-action model via instruction-driven routing & sparsification. *Advances in Neural Information Processing Systems*, 2025.
- Xinghang Li, Peiyan Li, Minghuan Liu, Dong Wang, Jirong Liu, Bingyi Kang, Xiao Ma, Tao Kong, Hanbo Zhang, and Huaping Liu. Towards generalist robot policies: What matters in building vision-language-action models. *arXiv preprint arXiv:2412.14058*, 2024a.
- Xinghang Li, Minghuan Liu, Hanbo Zhang, Cunjun Yu, Jie Xu, Hongtao Wu, Chilam Cheang, Ya Jing, Weinan Zhang, Huaping Liu, Hang Li, and Tao Kong. Vision-language foundation models as effective robot imitators. In *International Conference on Learning Representations*, 2024b.
- Bo Liu, Yifeng Zhu, Chongkai Gao, Yihao Feng, Qiang Liu, Yuke Zhu, and Peter Stone. Libero: Benchmarking knowledge transfer for lifelong robot learning. In *Thirty-seventh Conference on Neural Information Processing Systems Datasets and Benchmarks Track*, 2023. URL https://proceedings.neurips.cc/paper_files/paper/2023/hash/8c3c666820ea055a77726d66fc7d447f-Abstract-Datasets_and_Benchmarks.html.
- Shih-Yang Liu, Chien-Yi Wang, Hongxu Yin, Pavlo Molchanov, Yu-Chiang Frank Wang, Kwang-Ting Cheng, and Min-Hung Chen. Dora: Weight-decomposed low-rank adaptation. In *Proceedings of the 41st International Conference on Machine Learning*, volume 235 of *Proceedings of Machine Learning Research*, pages 32100–32121. PMLR, 2024. URL <https://proceedings.mlr.press/v235/liu24bn.html>.
- Zefang Liu and Jiahua Luo. Adamole: Fine-tuning large language models with adaptive mixture of low-rank adaptation experts. In *Conference on Language Modeling*, 2024.
- Yueen Ma, Zixing Song, Yuzheng Zhuang, Jianye Hao, and Irwin King. A survey on vision-language-action models for embodied ai. *arXiv preprint arXiv:2405.14093*, 2024.
- Oier Mees, Lukas Hermann, Erick Rosete-Beas, and Wolfram Burgard. Calvin: A benchmark for language-conditioned policy learning for long-horizon robot manipulation tasks. *IEEE Robotics and Automation Letters*, 7(3):7327–7334, 2022.
- Fanxu Meng, Zhaohui Wang, and Muhan Zhang. Pissa: Principal singular values and singular vectors adaptation of large language models. In *Advances in Neural Information Processing Systems*, volume 37, pages 121038–121072, 2024. doi: 10.52202/079017-3846. URL https://proceedings.neurips.cc/paper_files/paper/2024/hash/db36f4d603cc9e3a2a5e10b93e6428f2-Abstract-Conference.html.
- NVIDIA GEAR Team. GR00T N1.6: An improved open foundation model for generalist humanoid robots. https://research.nvidia.com/labs/gear/gr00t-n1_6/, 2025. Accessed: 2026-04-28.
- Abdullah Yahya Abdullah Omaisani and Ibrahim Sheikh Mohamed. Towards accessible physical ai: Lora-based fine-tuning of vla models for real-world robot control. *arXiv preprint arXiv:2512.11921*, 2025. URL <https://arxiv.org/abs/2512.11921>.
- Karl Pertsch, Kyle Stachowicz, Brian Ichter, Danny Driess, Suraj Nair, Quan Vuong, Oier Mees, Chelsea Finn, and Sergey Levine. Fast: Efficient action tokenization for vision-language-action models, 2025. URL <https://arxiv.org/abs/2501.09747>.

- Moritz Reuss, Hongyi Zhou, Marcel Rühle, Ömer Erdiñç Yağmurlu, Fabian Otto, and Rudolf Lioutikov. Flower: Democratizing generalist robot policies with efficient vision-language-flow models. In Joseph Lim, Shuran Song, and Hae-Won Park, editors, *Proceedings of The 9th Conference on Robot Learning*, volume 305 of *Proceedings of Machine Learning Research*, pages 3736–3761. PMLR, 27–30 Sep 2025. URL <https://proceedings.mlr.press/v305/reuss25a.html>.
- Mohit Shridhar, Lucas Manuelli, and Dieter Fox. Perceiver-actor: A multi-task transformer for robotic manipulation. In *Proceedings of The 6th Conference on Robot Learning*, volume 205 of *Proceedings of Machine Learning Research*, 2023.
- Shuhan Tan, Kairan Dou, Yue Zhao, and Philipp Krähenbühl. Interactive post-training for vision-language-action models, 2025. URL <https://arxiv.org/abs/2505.17016>.
- Chunlin Tian, Zhan Shi, Zhijiang Guo, Li Li, and Chengzhong Xu. Hydralora: An asymmetric lora architecture for efficient fine-tuning. *arXiv preprint arXiv:2404.19245*, 2024.
- Fan Wang, Juyong Jiang, Chansung Park, Sunghun Kim, and Jing Tang. Kasa: Knowledge-aware singular-value adaptation of large language models. *arXiv preprint arXiv:2412.06071*, 2024a.
- Hanqing Wang, Yixia Li, Shuo Wang, Guanhua Chen, and Yun Chen. Milora: Harnessing minor singular components for parameter-efficient llm finetuning. *arXiv preprint arXiv:2406.09044*, 2024b.
- Hanqing Wang, Yixia Li, Shuo Wang, Guanhua Chen, and Yun Chen. Milora: Harnessing minor singular components for parameter-efficient llm finetuning. In *Proceedings of the 2025 Conference of the Nations of the Americas Chapter of the Association for Computational Linguistics: Human Language Technologies (Volume 1: Long Papers)*, pages 4823–4836, Albuquerque, New Mexico, 2025. Association for Computational Linguistics. doi: 10.18653/v1/2025.naacl-long.248. URL <https://aclanthology.org/2025.naacl-long.248/>.
- Junjie Wen, Yichen Zhu, Minjie Zhu, Zhibin Tang, Jinming Li, Zhongyi Zhou, Xiaoyu Liu, Chaomin Shen, Yaxin Peng, and Feifei Feng. Diffusionvla: Scaling robot foundation models via unified diffusion and autoregression. In *Proceedings of the 42nd International Conference on Machine Learning*, volume 267 of *Proceedings of Machine Learning Research*, pages 66558–66574, 2025.
- Xiao-Ming Wu, Bin Fan, Kang Liao, Jian-Jian Jiang, Runze Yang, Yihang Luo, Zhonghua Wu, Wei-Shi Zheng, and Chen Change Loy. Vlanext: Recipes for building strong vla models. *arXiv preprint arXiv:2602.18532*, 2026.
- Shuai Yang, Hao Li, Bin Wang, Yilun Chen, Yang Tian, Tai Wang, Hanqing Wang, Feng Zhao, Yiyi Liao, and Jiangmiao Pang. Instructvla: Vision-language-action instruction tuning from understanding to manipulation. *arXiv preprint arXiv:2507.17520*, 2025.
- Yandan Yang, Shuang Zeng, Tong Lin, Xinyuan Chang, Dekang Qi, Junjin Xiao, Haoyun Liu, Ronghan Chen, Yuzhi Chen, Dongjie Huo, Feng Xiong, Xing Wei, Zhiheng Ma, and Mu Xu. Abot-m0: Vla foundation model for robotic manipulation with action manifold learning. *arXiv preprint arXiv:2602.11236*, 2026.
- Bin Yu, Shijie Lian, Xiaopeng Lin, Yuliang Wei, Zhaolong Shen, Changti Wu, Yuzhuo Miao, Xinming Wang, Bailing Wang, Cong Huang, and Kai Chen. Twinbrainvla: Unleashing the potential of generalist vlms for embodied tasks via asymmetric mixture-of-transformers. *arXiv preprint arXiv:2601.14133*, 2026.
- Ted Zadori, Ahmet Üstün, Arash Ahmadian, Beyza Ermiş, Acyr Locatelli, and Sara Hooker. Pushing mixture of experts to the limit: Extremely parameter efficient moe for instruction tuning. In *The Twelfth International Conference on Learning Representations*, 2024.
- Michał Zawalski, William Chen, Karl Pertsch, Oier Mees, Chelsea Finn, and Sergey Levine. Robotic control via embodied chain-of-thought reasoning. In Pulkit Agrawal, Oliver Kroemer, and Wolfram Burgard, editors, *Proceedings of The 8th Conference on Robot Learning*, volume 270 of *Proceedings of Machine Learning Research*, pages 3157–3181. PMLR, 06–09 Nov 2025. URL <https://proceedings.mlr.press/v270/zawalski25a.html>.
- Jianke Zhang, Xiaoyu Chen, Qiuyue Wang, Mingsheng Li, Yanjiang Guo, Yucheng Hu, Jiajun Zhang, Shuai Bai, Junyang Lin, and Jianyu Chen. Vlm4vla: Revisiting vision-language-models in vision-language-action models. *arXiv preprint arXiv:2601.03309*, 2026.
- Jinliang Zheng, Jianxiong Li, Zhihao Wang, Dongxiu Liu, Xirui Kang, Yuchun Feng, Yanan Zheng, Jiayin Zou, Yilun Chen, Jia Zeng, Ya-Qin Zhang, Jiangmiao Pang, Jingjing Liu, Tai Wang, and Xianyuan Zhan. X-vla: Soft-prompted transformer as scalable cross-embodiment vision-language-action model. *arXiv preprint arXiv:2510.10274*, 2025.

Brianna Zitkovich, Nikhil Joshi, Alex Irpan, Brian Ichter, Jasmine Hsu, Alexander Herzog, Karol Hausman, Keerthana Gopalakrishnan, Chuyuan Fu, Pete Florence, Chelsea Finn, Kumar Avinava Dubey, Danny Driess, Tianli Ding, Krzysztof Marcin Choromanski, Xi Chen, Yevgen Chebotar, Justice Carbajal, Noah Brown, Anthony Brohan, Montserrat Gonzalez Arenas, and Kehang Han. Rt-2: Vision-language-action models transfer web knowledge to robotic control. In *Proceedings of The 7th Conference on Robot Learning*, volume 229 of *Proceedings of Machine Learning Research*, pages 2165–2183, 2023.

A Technical Appendices and Supplementary Material

A.1 Limitations and Future Works

A limitation of the current study is that our evaluation is still restricted to robotics-oriented settings, including embodied policy learning and real-world manipulation tasks, and we have not yet validated the proposed framework in other multimodal domains that also require high precision, such as medical image analysis, financial market forecasting, or ancient literature restoration. Extending VLA-GSE to these also high-precision and multimodal domains is an important direction for future works, and would help clarify the generality of the generalized–specialized expert design beyond robotics. Despite this limitation, our main contribution is to present a simple, parameter-efficient, and effective adaptation framework that improves robustness and transfer in robotic VLA learning.

A.2 Statement for Use of LLMs

LLMs were only used to assist with language polishing in certain sections of this paper.

A.3 Reproducibility Statement

We provide open-source code to reproduce all experiments. To facilitate reproducibility, we additionally include a minimal working example and environment setup instructions, enabling researchers to verify correctness and replicate our reported results with minimal effort. Code is available at <https://github.com/YuhuaJiang2002/VLA-GSE>.

A.4 Impact Statement

This paper presents work whose goal is to advance the field of machine learning. We do not identify any specific impacts of this work that require particular emphasis here.

B Proof of Theorem 1

Proof. For the i -th specialized expert, its effective contribution to the aggregated equivalent weight is $w^i(x)W_s^i$, where $W_s^i = s_s^i B_s^i A_s^i$. Let $g = \frac{\partial \mathcal{L}_{\text{final}}}{\partial W_{\text{eq}}(x)}$ denote the gradient of the loss with respect to the aggregated equivalent weight. By the chain rule, the localized gradients with respect to A_s^i and B_s^i are

$$g_A^i = \frac{\partial \mathcal{L}_{\text{final}}}{\partial A_s^i} = \frac{\partial (w^i(x)W_s^i)}{\partial A_s^i} \frac{\partial \mathcal{L}_{\text{final}}}{\partial (w^i(x)W_s^i)} = w^i(x) s_s^i (B_s^i)^\top g, \quad (13)$$

$$g_B^i = \frac{\partial \mathcal{L}_{\text{final}}}{\partial B_s^i} = \frac{\partial \mathcal{L}_{\text{final}}}{\partial (w^i(x)W_s^i)} \frac{\partial (w^i(x)W_s^i)}{\partial B_s^i} = w^i(x) s_s^i g (A_s^i)^\top. \quad (14)$$

Using the initialization

$$B_s^i = \sqrt{\frac{1}{s_s^i}} U_i \Sigma_i^{1/2}, \quad A_s^i = \sqrt{\frac{1}{s_s^i}} \Sigma_i^{1/2} V_i^\top, \quad (15)$$

we obtain

$$g_A^i = w^i(x) s_s^i \left(\sqrt{\frac{1}{s_s^i}} U_i \Sigma_i^{1/2} \right)^\top g = w^i(x) \sqrt{s_s^i} \Sigma_i^{1/2} U_i^\top g, \quad (16)$$

$$g_B^i = w^i(x) s_s^i g \left(\sqrt{\frac{1}{s_s^i}} \Sigma_i^{1/2} V_i^\top \right)^\top = w^i(x) \sqrt{s_s^i} g V_i \Sigma_i^{1/2}. \quad (17)$$

We first analyze the squared Frobenius norm of g_A^i :

$$\begin{aligned}\|g_A^i\|_F^2 &= \text{Tr}((g_A^i)^\top g_A^i) \\ &= \text{Tr}\left(\left(w^i(x) \sqrt{s_s^i} \Sigma_i^{1/2} U_i^\top g\right)^\top \left(w^i(x) \sqrt{s_s^i} \Sigma_i^{1/2} U_i^\top g\right)\right) \\ &= (w^i(x))^2 s_s^i \text{Tr}(g^\top U_i \Sigma_i U_i^\top g).\end{aligned}\quad (18)$$

Taking expectation over the training batch distribution and using the cyclic property of the trace gives

$$\mathbb{E}[\|g_A^i\|_F^2] = s_s^i \mathbb{E}[(w^i(x))^2 \text{Tr}(g^\top U_i \Sigma_i U_i^\top g)]. \quad (19)$$

To analyze the expected squared gradient norm, we consider the idealized balanced-routing condition and define

$$\rho_w := \mathbb{E}[(w^i(x))^2]. \quad (20)$$

Under balanced routing, ρ_w is identical across experts and thus does not depend on i . Therefore, when taking expectations of $\|g_A^i\|_F^2$ or $\|g_B^i\|_F^2$, the routing term contributes only the same multiplicative factor ρ_w for all experts. As a result, it does not affect the relative scaling across experts, and the trace-inverse scaling rule remains unchanged. Absorbing this shared routing second-moment factor, we obtain

$$\begin{aligned}\mathbb{E}[\|g_A^i\|_F^2] &= \rho_w s_s^i \text{Tr}(U_i \Sigma_i U_i^\top \mathbb{E}[gg^\top]) \\ &= \rho_w s_s^i \text{Tr}(\Sigma_i U_i^\top G_L U_i).\end{aligned}\quad (21)$$

Define

$$\alpha_i^L = \text{Tr}(\Sigma_i U_i^\top G_L U_i). \quad (22)$$

Then Eq. (21) becomes

$$\mathbb{E}[\|g_A^i\|_F^2] = \rho_w s_s^i \alpha_i^L. \quad (23)$$

We next analyze g_B^i . From Eq. (17),

$$\begin{aligned}\|g_B^i\|_F^2 &= \text{Tr}((g_B^i)^\top g_B^i) \\ &= \text{Tr}\left(\left(w^i(x) \sqrt{s_s^i} g V_i \Sigma_i^{1/2}\right)^\top \left(w^i(x) \sqrt{s_s^i} g V_i \Sigma_i^{1/2}\right)\right) \\ &= (w^i(x))^2 s_s^i \text{Tr}(\Sigma_i V_i^\top g^\top g V_i).\end{aligned}\quad (24)$$

Taking expectation yields

$$\begin{aligned}\mathbb{E}[\|g_B^i\|_F^2] &= s_s^i \mathbb{E}[(w^i(x))^2 \text{Tr}(\Sigma_i V_i^\top g^\top g V_i)] \\ &= \rho_w s_s^i \text{Tr}(\Sigma_i V_i^\top \mathbb{E}[g^\top g] V_i) \\ &= \rho_w s_s^i \text{Tr}(\Sigma_i V_i^\top G_R V_i).\end{aligned}\quad (25)$$

Define

$$\alpha_i^R = \text{Tr}(\Sigma_i V_i^\top G_R V_i). \quad (26)$$

Then Eq. (25) becomes

$$\mathbb{E}[\|g_B^i\|_F^2] = \rho_w s_s^i \alpha_i^R. \quad (27)$$

Equations (23) and (27) prove the first part of the theorem under the idealized balanced-routing assumption at initialization. Since ρ_w is shared across experts, it does not affect the relative scaling across experts, and thus does not change the trace-inverse scaling rule derived below.

We now prove the trace-inverse scaling rule. Assume there exist constants $\kappa_L, \kappa_R > 0$ such that²

$$\alpha_i^L = \kappa_L \text{Tr}(\Sigma_i), \quad \alpha_i^R = \kappa_R \text{Tr}(\Sigma_i), \quad \forall i \in \{1, \dots, E\}. \quad (28)$$

Substituting Eq. (28) into Eqs. (23) and (27), we obtain

$$\mathbb{E}[\|g_A^i\|_F^2] = \rho_w s_s^i \kappa_L \text{Tr}(\Sigma_i), \quad (29)$$

$$\mathbb{E}[\|g_B^i\|_F^2] = \rho_w s_s^i \kappa_R \text{Tr}(\Sigma_i). \quad (30)$$

²This assumption is automatically satisfied under $G_L = \mathbb{E}[gg^\top] \propto I$ and $G_R = \mathbb{E}[g^\top g] \propto I$, which is the commonly used isotropic gradient variance assumption [used in Theorem 1 of Jastrzebski et al., 2018].

Therefore, if we choose

$$s_s^i = s_{\text{base}} \cdot \frac{C}{\text{Tr}(\Sigma_i)}, \quad (31)$$

then it follows that

$$\mathbb{E}[\|g_A^i\|_F^2] = \rho_w s_{\text{base}} C \kappa_L, \quad (32)$$

$$\mathbb{E}[\|g_B^i\|_F^2] = \rho_w s_{\text{base}} C \kappa_R, \quad (33)$$

which are independent of i . Hence, the expected squared Frobenius norms of the localized gradients are equalized across all specialized experts. This proves the theorem. \square

Proposition 2 (Isotropic global gradient variance implies projected uniformity). *A sufficient condition for the projected-uniformity condition in Eq. (28) is that the global gradient second moments are isotropic, namely*

$$G_L = \mathbb{E}[gg^\top] = c_L I, \quad G_R = \mathbb{E}[g^\top g] = c_R I, \quad (34)$$

for some constants $c_L, c_R > 0$. Under this assumption, for every specialized expert i ,

$$\alpha_i^L = c_L \text{Tr}(\Sigma_i), \quad \alpha_i^R = c_R \text{Tr}(\Sigma_i), \quad (35)$$

where

$$\alpha_i^L = \text{Tr}(\Sigma_i U_i^\top G_L U_i), \quad \alpha_i^R = \text{Tr}(\Sigma_i V_i^\top G_R V_i). \quad (36)$$

Therefore, Eq. (28) holds with $\kappa_L = c_L$ and $\kappa_R = c_R$.

Proof. Since U_i and V_i are composed of orthogonal singular vectors, they satisfy $U_i^\top U_i = I$ and $V_i^\top V_i = I$. Substituting $G_L = c_L I$ into α_i^L gives

$$\alpha_i^L = \text{Tr}(\Sigma_i U_i^\top (c_L I) U_i) = c_L \text{Tr}(\Sigma_i U_i^\top U_i) = c_L \text{Tr}(\Sigma_i). \quad (37)$$

Similarly, substituting $G_R = c_R I$ into α_i^R yields

$$\alpha_i^R = \text{Tr}(\Sigma_i V_i^\top (c_R I) V_i) = c_R \text{Tr}(\Sigma_i V_i^\top V_i) = c_R \text{Tr}(\Sigma_i). \quad (38)$$

Hence the projected-uniformity condition is satisfied exactly with $\kappa_L = c_L$ and $\kappa_R = c_R$. This isotropic case is a standard analytically tractable setting in the optimization literature for studying gradient-based methods [see Theorem 1 of Jastrzębski et al., 2018]. \square

C Proof of Expectation-Based Backbone Weight Adjustment

Proof. Recall that the effective weight of the proposed module is

$$W_{eq}(x) = \tilde{W}_0 + s_g B_g A_g + \sum_{i=1}^E w^i(x) s_s^i B_s^i A_s^i, \quad (39)$$

where \tilde{W}_0 is defined as

$$\tilde{W}_0 = W_0 - s_g B_g A_g - \frac{1}{E} \sum_{i=1}^E s_s^i B_s^i A_s^i. \quad (40)$$

Under the uniform-routing assumption at initialization, each specialized expert is selected with equal probability in expectation. Hence,

$$\mathbb{E}_x[w^i(x)] = \frac{1}{E}, \quad i = 1, \dots, E. \quad (41)$$

Therefore, taking expectation over the input-dependent routing gives

$$\begin{aligned} \mathbb{E}_x[W_{eq}(x)] &= \tilde{W}_0 + s_g B_g A_g + \mathbb{E}_x \left[\sum_{i=1}^E w^i(x) s_s^i B_s^i A_s^i \right] \\ &= \tilde{W}_0 + s_g B_g A_g + \sum_{i=1}^E \mathbb{E}_x[w^i(x)] s_s^i B_s^i A_s^i \\ &= \tilde{W}_0 + s_g B_g A_g + \frac{1}{E} \sum_{i=1}^E s_s^i B_s^i A_s^i. \end{aligned} \quad (42)$$

Substituting the definition of \tilde{W}_0 yields

$$\mathbb{E}_x[W_{eq}(x)] = W_0. \quad (43)$$

Thus, the effective weight $W_{eq}(x)$ is aligned with the original backbone weight W_0 in expectation at initialization. \square

D More Experiment Results

D.1 More Qualitative Evaluation in Generalization Scenarios

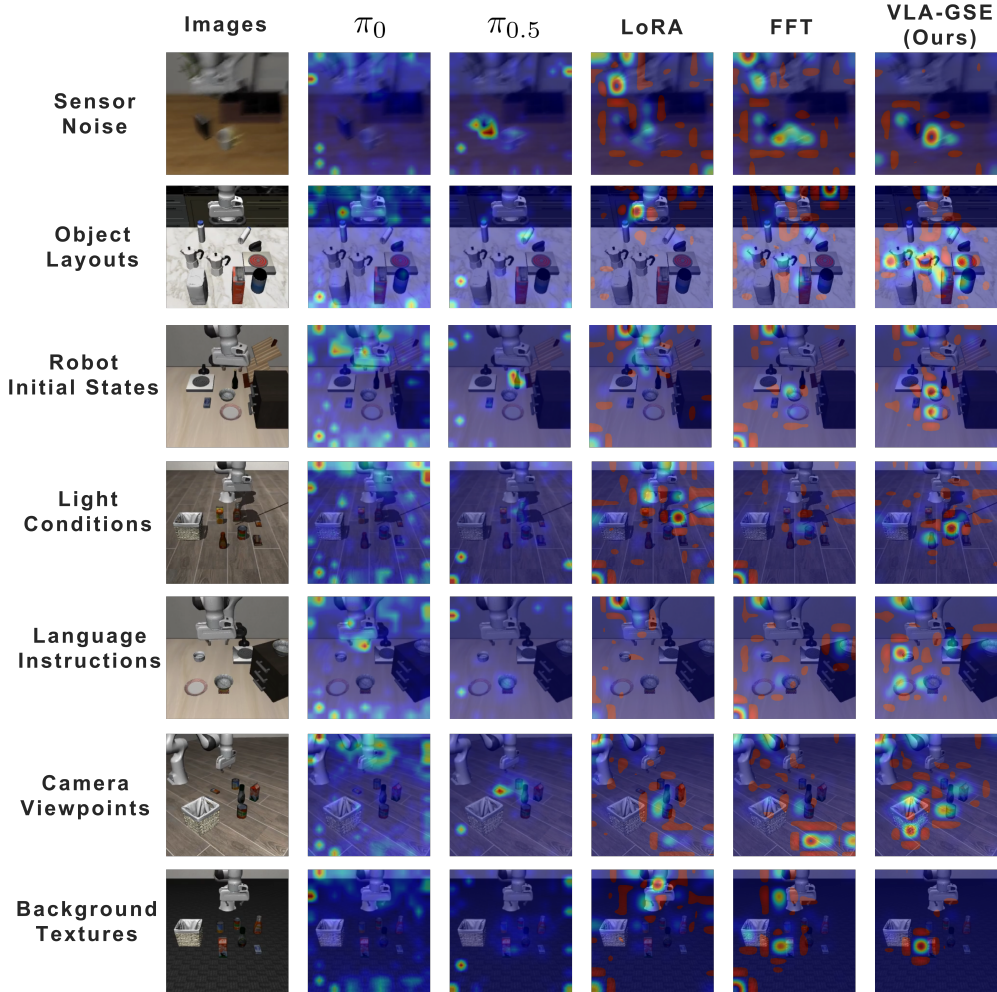


Figure 4: Extended attention map visualizations under seven diverse generalization scenarios. As a comprehensive supplement to the main text, this figure demonstrates the robustness of our VLA-GSE method across variations in Camera Viewpoints, Object Layouts, Robot Initial States, Light Conditions, Language Instructions, Sensor Noise, and Background Textures. All attention maps are taken from the last transformer layer of the models. GSE consistently maintains precise attention on the graspable edges of target objects, while baseline models (π_0 , $\pi_{0.5}$, LoRA, and FFT) suffer from severe visual distractions or become unfocused under domain shifts.

As a comprehensive supplement to the qualitative evaluation presented in the main text, Figure 4 provides an extensive visualization of model attention maps across a wider range of out-of-distribution (OOD) generalization scenarios. Specifically, we evaluate the visual grounding robustness of all models under seven challenging axes of variation: Camera Viewpoints, Object Layouts, Robot Initial States, Light Conditions, Language Instructions, Sensor Noise, and Background Textures. All attention maps are taken from the last transformer layer of the models.

Table 6: LIBERO simulation benchmark results. Success rates (SR, %) across the four LIBERO task suites.

Method	Spatial	Object	Goal	Long	Average
Diffusion Policy [Chi et al., 2023]	78.3	92.5	68.3	50.5	72.4
Dita [Hou et al., 2025]	97.4	94.8	93.2	83.6	92.3
π_0 [Black et al., 2025b]	96.8	98.8	95.8	85.2	94.2
$\pi_{0.5}$ [Black et al., 2025a]	98.8	98.2	98.0	92.4	96.9
FLOWER [Reuss et al., 2025]	97.5	99.1	96.1	94.9	96.9
GR00T-N1.6 [NVIDIA GEAR Team, 2025]	97.7	98.5	97.5	94.4	97.0
OpenVLA-OFT [Kim et al., 2025a]	97.6	98.4	97.9	94.5	97.1
CogVLA [Li et al., 2025]	98.6	98.8	96.6	95.4	97.4
VLANeXt [Wu et al., 2026]	99.0	99.2	96.6	94.6	97.4
X-VLA [Zheng et al., 2025]	98.2	98.6	97.8	97.6	98.1
VLA-GSE (Ours)	98.8	99.8	98.2	96.8	98.4

The results in Figure 4 consistently corroborate our previous findings and further highlight the exceptional generalization capabilities of our proposed GSE method. Across all seven diverse visual domain shifts, GSE stably and precisely focuses its attention on the relevant target objects and their critical graspable edges. This remarkable robustness empirically validates our core motivation: by effectively preserving the broad, pre-trained visual knowledge of the base Qwen3-VL model, GSE inherits its strong invariance to environmental variations (such as lighting changes, background shifts, and sensor noise). Concurrently, the efficiently learned manipulation skills allow GSE to accurately pinpoint the optimal affordance regions regardless of the scene layout or camera angle.

Conversely, the baseline models exhibit significant fragility when faced with these generalization scenarios. π_0 consistently demonstrates scattered and uninformative attention distributions across all settings. While $\pi_{0.5}$, LoRA, and FFT show localized attention in some specific cases, their performance drastically degrades under severe domain shifts (e.g., sensor noise or complex background textures). In these challenging settings, the baselines either completely lose track of the objects or severely overfit to spurious background features and incorrect distractors. This widespread failure among the standard fine-tuning and basic PEFT baselines strongly implies that they suffer from catastrophic forgetting, losing the base VLM’s inherent visual robustness during the adaptation to robotic tasks. In contrast, GSE successfully bridges the gap between robust, general-purpose visual understanding and precise, task-specific action execution.

D.2 Comparison of VLA Models on LIBERO Results

Table 6 reports the simulation results on LIBERO. VLA-GSE achieves the best overall performance, reaching an average success rate of 98.4%. Even after including strong recent baselines such as FLOWER, GR00T-N1.6, VLANeXt, and X-VLA, our method still ranks first overall, outperforming the strongest baseline, X-VLA, by 0.3 points in average success rate. VLA-GSE also establishes new best results on Object (99.8%) and Goal (98.2%), while remaining highly competitive on Spatial (98.8%) and Long (96.8%).

These results suggest that GSE provides a strong balance between fine-grained task adaptation and robustness across heterogeneous task suites. In particular, compared with X-VLA, the gains on Object and Goal are +1.2 and +0.4 points, respectively, indicating that the proposed generalized-specialized expert decomposition improves task-specific adaptation without sacrificing cross-suite generalization. Although VLANeXt attains the best Spatial score and X-VLA achieves the best Long score, VLA-GSE delivers the highest average performance, demonstrating the strongest overall trade-off across the four LIBERO suites. Overall, the results show that parameter-efficient adaptation with generalized and specialized experts can remain competitive with, and often surpass, strong recent VLA baselines without requiring full-model fine-tuning.

Table 7: Fine-tuning method comparison on the standard LIBERO benchmark. Results are reported as success rate (%) across the four task suites. All PEFT methods are configured with comparable trainable parameter budgets, following the setting in Table 2.

Method	Params (%)	Spatial	Object	Goal	Long	Average
FFT (Full Fine-Tuning)	100.00	97.8	98.8	96.4	94.2	96.8
LoRA [Hu et al., 2022]	2.58	94.4	96.8	90.4	78.4	90.0
MiLoRA [Wang et al., 2025]	2.52	97.0	98.2	95.0	84.2	93.6
PiSSA [Meng et al., 2024]	2.54	96.0	97.4	93.6	89.8	94.2
rsLoRA [Kalajdziewski, 2023]	2.52	96.4	98.0	94.0	90.8	94.8
HydraLoRA [Tian et al., 2024]	2.55	96.6	98.0	94.2	91.2	95.0
DoRA [Liu et al., 2024]	2.54	96.6	98.2	94.4	91.6	95.2
AdaMoLE [Liu and Luo, 2024]	2.53	96.8	98.2	94.8	91.8	95.4
MoLoRA [Zadouri et al., 2024]	2.56	97.2	98.4	95.2	92.4	95.8
GOAT [Fan et al., 2025]	2.54	97.4	98.6	95.8	93.0	96.2
VLA-GSE (Ours)	2.51	98.8	99.8	98.2	96.8	98.4

D.3 Comparison of Fine-Tuning Methods on LIBERO Results

Table 7 reports the results on the standard LIBERO benchmark. Overall, the ranking is broadly consistent with that on LIBERO-Plus: stronger parameter-efficient fine-tuning methods on zero-shot generalization also tend to achieve better performance on the in-distribution LIBERO benchmark. Vanilla low-rank adaptation, such as LoRA, already provides a competitive baseline, while more advanced variants, including DoRA, AdaMoLE, MoLoRA, and GOAT, further improve the average success rate, indicating that a richer adaptation space is beneficial even under the standard simulation setting.

Among all baselines, FFT remains highly competitive, achieving an average success rate of 96.8%. Nevertheless, VLA-GSE still delivers the strongest overall performance, reaching 98.4% average success rate and ranking first on all four suites. Compared with FFT, our method improves Spatial from 97.8% to 98.8%, Object from 98.8% to 99.8%, Goal from 96.4% to 98.2%, and Long from 94.2% to 96.8%, corresponding to gains of 1.0, 1.0, 1.8, and 2.6 points, respectively. The largest improvement is observed on the Long suite, suggesting that VLA-GSE is particularly effective for long-horizon manipulation requiring sustained temporal consistency and accurate multi-step action composition.

Compared with the strongest PEFT baseline, GOAT, VLA-GSE improves the average success rate from 96.2% to 98.4%, yielding a margin of 2.2 points. This advantage is again most pronounced on the more challenging Goal and Long suites, where our method outperforms GOAT by 2.4 and 3.8 points, respectively. Notably, Object is already close to saturation for most competitive methods, whereas Long still exhibits a clear performance spread. This pattern indicates that long-horizon sequential manipulation remains the main differentiating factor once short-horizon perception and control are well handled. Overall, these results provide additional evidence that explicitly combining generalized transferable adaptation with specialized experts yields a more effective fine-tuning mechanism for VLAs than both conventional LoRA-style methods and existing LoRA-MoE variants.

D.4 Real-World Inference Time Comparison

We further compare the real-world inference efficiency of different policies by measuring the wall-clock latency required to generate one action chunk. All methods are evaluated with batch size 1 under the same deployment pipeline on the same real-robot workstation equipped with an NVIDIA RTX 5080 GPU. We measure the elapsed time from receiving the current observation to returning the full action chunk, and report the average latency over 120 runs.

As shown in Figure 5, Qwen3-VL-FFT achieves the lowest latency, while VLA-GSE is the second fastest method among the compared policies. The most controlled comparison is between VLA-GSE and Qwen3-VL-FFT, since both are built on the same Qwen3-VL-4B backbone and mainly differ in the adaptation strategy. Under this matched setting, the latency gap indicates that the proposed generalized-specialized expert design introduces only a modest additional inference overhead.

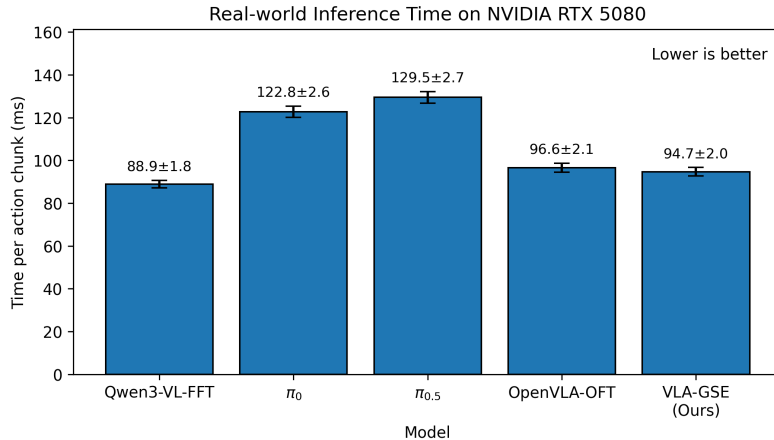


Figure 5: Real-world inference latency comparison on an NVIDIA RTX 5080 GPU. We report the wall-clock time for generating one action chunk with batch size 1. Error bars denote standard deviation over 120 runs. Lower is better.

Table 8: Suite-wise zero-shot performance of VLA-GSE on LIBERO-Plus. Results are shown in success rate (%).

Suite	Camera	Robot	Language	Light	Background	Noise	Layout	Total
Spatial	89.5	80.6	89.6	94.8	96.4	89.2	95.2	90.3
Object	80.5	65.3	95.1	100.0	98.4	86.6	85.1	86.2
Goal	51.7	67.2	79.3	99.6	96.1	76.5	62.8	74.2
Long	35.8	61.0	91.0	94.9	98.3	65.2	87.3	74.1
Average	64.4	68.5	88.8	97.3	97.3	79.4	82.6	81.2

We note, however, that absolute latency comparisons across different policy families should be interpreted with caution. In particular, the lower latency of VLA-GSE relative to π_0 and $\pi_{0.5}$ is not solely due to the proposed adapter design, but also reflects differences in the action-generation paradigm: VLA-GSE adopts OFT-style parallel decoding, whereas π_0 and $\pi_{0.5}$ rely on flow-matching-based generation, which is inherently more expensive at inference time. Similarly, the lower latency of VLA-GSE relative to OpenVLA-OFT should not be over-interpreted as a pure architectural advantage of GSE, since OpenVLA-OFT is built on a larger 7B backbone, whereas VLA-GSE uses a 4B backbone. Therefore, these cross-model comparisons are best viewed as end-to-end deployment measurements rather than clean isolation of module-level efficiency.

Overall, the main takeaway from Figure 5 is that, relative to the matched Qwen3-VL-FFT baseline, VLA-GSE improves policy performance while incurring only a small additional inference-time cost, while remaining practically efficient for real-world deployment.

D.5 Suite-wise Results on LIBERO-Plus

For compact comparison, tables in the main paper reports only the averaged LIBERO-Plus performance of VLA-GSE. Here, we provide its detailed zero-shot results on the four LIBERO suites: *Spatial*, *Object*, *Goal*, and *Long*.

As shown in Table 8, VLA-GSE achieves strong performance across all four suites, with the best overall results on *Spatial* (90.3) and competitive performance on the more challenging *Goal* and *Long* suites. Notably, the suite-wise breakdown shows that the strong averaged performance in the main paper is not dominated by a single suite, but is supported by consistently high robustness across diverse distribution shifts, including camera, robot embodiment, language, lighting, background, noise, and layout variations. These results further demonstrate that VLA-GSE generalizes well across different task structures and evaluation conditions in LIBERO-Plus.

D.6 Training Details, Hyperparameters, and Task Description

Training Details and Hyperparameters Table 9 details the comprehensive set of hyperparameters and training configurations used for fine-tuning the Qwen3-VL-4B-Instruct VLM with our proposed VLA-GSE framework.

Real-World Task Description and Hyperparameters For the real-world experiments, we evaluate four representative long-horizon manipulation tasks: *pour water into bowl*, which requires stable container grasping and controlled pouring; *pick spoon into plate*, which involves precise grasping and object placement; *put carrot into bowl*, which tests visually grounded pick-and-place under object-level spatial variation; and *take pen out of pen container*, which requires extracting a slender pen from a cylindrical container. For each task, we collect 70 in-distribution demonstrations via teleoperation. Each task contains 60 evaluation episodes, covering four out-of-distribution (OOD) generalization settings: variations in *lighting*, which change scene illumination conditions; *language*, which rephrase the task instruction; *clutter layout*, which modify the arrangement of surrounding objects; and *background tablecloth*, which alter the background appearance of the workspace. These settings are designed to evaluate the robustness of the learned policy under realistic visual and linguistic distribution shifts.

During training, we set the learning rate for the VLM and GSE parameters to 1×10^{-5} , and the learning rate for the action MLP head to 1×10^{-4} . The policy for *pour water into bowl* is trained for 8000 iterations, whereas the policies for the other three tasks are each trained for 6000 iterations. Other real-world task training details and hyperparameters are consistent with Table 9.

E VLA-GSE Algorithm Pseudo-code

In this section, we provide the complete pseudo-code for the VLA-GSE framework. Algorithm 1 explicitly outlines the two primary operational phases of our approach. The first phase is the SVD-based adaptive initialization, where the pre-trained weight matrix is decomposed. The dominant singular values are allocated to the generalized expert to anchor foundational knowledge, while the subsequent singular components are partitioned among the specialized experts. A crucial element of this phase is the backbone weight adjustment scheme via residual subtraction, which preemptively deducts the expected initial contribution of the newly added experts from the pre-trained backbone. The second phase details the forward pass, which aggregates the adjusted frozen weights, the continuously active generalized expert, and the dynamically routed top- k specialized experts.

F Catastrophic Forgetting under VLM-to-VLA Full-Parameter Fine-Tuning

A growing body of recent work has pointed out that directly adapting a pretrained VLM into a VLA by full-parameter fine-tuning can easily induce *catastrophic forgetting*. Although the VLM-to-VLA paradigm is attractive because it transfers rich visual-semantic priors from internet-scale pretraining to embodied control, the optimization objective in robot learning is substantially narrower than that of the original VLM. As a result, the backbone can over-specialize to low-level action prediction and partially lose the open-world understanding ability that originally motivated using a VLM backbone in the first place.

Several recent studies provide direct evidence for this phenomenon. Hancock et al. [2025] argue that catastrophic forgetting in VLM-to-VLA transfer is fundamentally related to the distribution mismatch between web-scale VLM pretraining data and robotics fine-tuning data. They show that learning to generate actions often diminishes the VLM’s original reasoning and multimodal understanding ability, which in turn harms semantic generalization and instruction following. Their solution is primarily *data-centric*: by re-expressing actions as language, they reduce representational mismatch and enable LoRA-based adaptation without heavily perturbing the pretrained backbone.

Dey et al. [2024] provide complementary evidence from the vision backbone perspective. Focusing on OpenVLA, they show that fine-tuning the full robotic model can lead to severe forgetting in the visual encoders, especially DINO-v2. In particular, they demonstrate that the DINO-v2 encoder inside OpenVLA fails on depth regression after VLA training, in sharp contrast to the original pretrained backbone. Their findings suggest that end-to-end robotic fine-tuning may overwrite core

Table 9: Hyperparameters and Configuration for VLA-GSE Fine-tuning

Hyperparameter / Setting	Value
<i>Architecture & VLA-GSE Configuration</i>	
Base VLM Backbone	Qwen3-VL-4B-Instruct
Action Head	OpenVLA-OFT MLP [Kim et al., 2025a]
Rank (r)	16
Rank of Generalized Expert (r_g)	2
Rank of Specialized Expert (d)	2
Total Experts per GSE Block	8
Generalized Experts	1
Top- k Routing	2
Router Initialization	Random Gaussian Noise
Initialization Type	SVD-based GSE
Total Generalized Experts in Model	356
Total Specialized Experts in Model	2492
<i>Training & Optimization</i>	
Training Dataset	LIBERO Benchmark (all 4 suites)
Total Optimization Steps	80,000
Batch Size per GPU	16
Total Effective Batch Size	128
Learning Rate (VLM / GSE Params)	1×10^{-5}
Learning Rate (Action MLP Head)	1×10^{-4}
Auxiliary Loss Weight (α)	0.01
Generalized Scaling Factor (s_g)	2
Specialized Scaling Factor (s_s^i)	$\frac{2 \cdot \sum_{j=1}^E \text{Tr}(\Sigma_j)}{E \cdot \text{Tr}(\Sigma_i)}$
Hardware	$8 \times$ NVIDIA A100 GPUs
<i>Parameter Efficiency</i>	
Total Parameters	4,551.85 M
Frozen Parameters (Non-GSE)	4,437.82 M
Trainable Parameters (Total)	114.04 M (2.51%)
Trainable Parameters (GSE Modules)	48.41 M
Trainable Parameters (Action Head)	65.62 M

spatial representations required for visual generalization. Their remedy is *post hoc restoration*: they partially revert the visual encoders back to their pretrained states through backbone reversal and model merging.

Yang et al. [2025] further observe that existing VLA models often suffer catastrophic forgetting of pretrained vision-language capabilities when adapted to manipulation. Their analysis shows that directly fine-tuning OpenVLA on instruction-rich embodied data yields limited gains on reasoning-intensive tasks because the original vision-language competence is not well preserved. To address this, they propose a *training-centric* solution based on joint multimodal instruction tuning, where embodied data and general multimodal data are optimized together.

Most strikingly, Yu et al. [2026] provide explicit empirical analysis of the severity of forgetting during VLA training. They report that standard robot-only VLA fine-tuning can cause a near-complete collapse of general visual understanding; for example, the POPE score of Qwen3-VL drops from 88.87% to 0.04% after fine-tuning. They also show that simple co-training with general visual QA data only partially alleviates the issue. Their proposed solution is therefore *architectural decoupling*: a frozen “Left Brain” preserves general semantic understanding, while a trainable “Right Brain” specializes in embodied control.

Our proposed VLA-GSE differs from the above lines of work in an important way. Rather than addressing forgetting primarily through data relabeling, co-training, post-training reversal, or duplicating the backbone into separate frozen/trainable branches, we approach the problem from the

Algorithm 1 GSE: Generalized and Specialized Experts Initialization and Forward Pass

Require: Input x , pre-trained weight W_0 , rank r_g for the generalized expert, rank d for specialized experts, number of specialized experts E , generalized scaling factor s_g , and specialized scaling factors $\{s_s^i\}_{i=1}^E$

- 1: **Initialization Phase:**
- 2: Compute SVD: $W_0 = U\Sigma V^\top$
- 3: ▷ 1. Initialize generalized expert (largest singular values)
- 4: $B_g \leftarrow \sqrt{\frac{1}{s_g}} U_{1:r_g} \Sigma_{1:r_g}^{1/2}$
- 5: $A_g \leftarrow \sqrt{\frac{1}{s_g}} \Sigma_{1:r_g}^{1/2} (V_{1:r_g})^\top$
- 6: ▷ 2. Initialize specialized experts (subsequent singular values)
- 7: **for** $i = 1$ to E **do**
- 8: Extract the i -th SVD segment $(U_i, \Sigma_i, V_i^\top)$ of rank d , starting after index r_g
- 9: $B_s^i \leftarrow \sqrt{\frac{1}{s_s^i}} U_i \Sigma_i^{1/2}$
- 10: $A_s^i \leftarrow \sqrt{\frac{1}{s_s^i}} \Sigma_i^{1/2} V_i^\top$
- 11: **end for**
- 12: ▷ 3. Backbone weight adjustment via residual subtraction
- 13: $W_{\text{res}} \leftarrow s_g B_g A_g + \frac{1}{E} \sum_{i=1}^E s_s^i B_s^i A_s^i$
- 14: $\tilde{W}_0 \leftarrow W_0 - W_{\text{res}}$
- 15: **return** $\tilde{W}_0, B_g, A_g, \{B_s^i, A_s^i\}_{i=1}^E$

- 16: **Forward Pass Phase**(x):
- 17: Compute gating scores $w^i(x)$ for specialized experts
- 18: Select top- k specialized experts $\Omega_k(x)$
- 19: $y_{\text{gen}} \leftarrow s_g B_g A_g x$
- 20: $y_{\text{spec}} \leftarrow \sum_{i \in \Omega_k(x)} w^i(x) s_s^i B_s^i A_s^i x$
- 21: **return** $\tilde{W}_0 x + y_{\text{gen}} + y_{\text{spec}}$

perspective of *architectural improvement within the adaptation module itself*. Concretely, VLA-GSE is built on the hypothesis that the tension between general visual-semantic knowledge and task-specific embodied adaptation should be handled by a better parameterization of the trainable update, rather than by fully rewriting the backbone. The generalized expert is designed to preserve and reuse dominant pretrained directions that support broad transferable capability, while the specialized experts allocate dedicated capacity for task-dependent embodied adaptation. This design aims to improve specialization without forcing the backbone update to collapse into a single monolithic fine-tuning trajectory.

Therefore, compared with prior methods, VLA-GSE is not merely a forgetting *mitigation strategy* added on top of standard adaptation; it is an architectural reformulation of the adaptation process itself. In this sense, our method is conceptually closer to improving the *structure of transfer* than to modifying the training data distribution or repairing forgetting after it has already occurred. We believe this distinction is important: it suggests that preserving general VLM capability and acquiring embodied expertise need not be treated as a purely training-data trade-off, but can instead be addressed through a more suitable model architecture for VLM-to-VLA transfer.

G Detailed Explanation of the Load Balancing Auxiliary Loss

Each GSE block adopts sparse routing over the specialized experts, which enables input-dependent adaptation while preserving computational efficiency. However, sparse top- k routing is known to suffer from a degenerate optimization behavior in which only a small subset of experts is selected for most tokens, whereas the remaining experts receive little gradient signal. This *routing collapse* effect reduces the effective capacity of the expert pool and weakens the intended specialization mechanism. To mitigate this issue, we introduce an auxiliary load-balancing objective following prior sparse MoE literature [Dai et al., 2024, Fedus et al., 2022].

We emphasize that this regularizer is imposed only on the routed specialized experts. The *Generalized Expert* is always activated and therefore does not participate in the routing competition.

For the l -th GSE block, consider a batch of T tokens with token representations $\{x^{(t)}\}_{t=1}^T$. Let $\Omega_k(x^{(t)})$ denote the set of top- k selected specialized experts for token $x^{(t)}$, and let $p^i(x^{(t)})$ denote the corresponding soft routing probability of expert i . We define the empirical selection frequency of expert i as

$$f_i^{(l)} = \frac{1}{T} \sum_{t=1}^T \mathbb{I}(i \in \Omega_k(x^{(t)})), \quad (44)$$

which measures how often expert i is actually activated under hard routing. In parallel, we define the average routing mass of expert i as

$$P_i^{(l)} = \frac{1}{T} \sum_{t=1}^T p^i(x^{(t)}), \quad (45)$$

which reflects the router’s continuous preference for that expert before the top- k truncation.

The auxiliary balancing term for block l is then given by

$$\mathcal{L}_{bal}^{(l)} = E \sum_{i=1}^E f_i^{(l)} P_i^{(l)}, \quad (46)$$

where E is the number of specialized experts. This form couples the hard assignment statistics $f_i^{(l)}$ with the soft routing scores $P_i^{(l)}$, and therefore penalizes imbalance at both the discrete and probabilistic levels. In particular, if the router collapses onto a small number of experts, then both $f_i^{(l)}$ and $P_i^{(l)}$ concentrate on those experts, leading to a larger penalty. Conversely, when expert usage is more evenly distributed, both quantities become closer to uniform and the regularizer is correspondingly reduced.

The overall training objective is

$$\mathcal{L} = \|\hat{a} - a\|_1 + \alpha \sum_{l=1}^L \mathcal{L}_{bal}^{(l)}, \quad (47)$$

where $\|\hat{a} - a\|_1$ denotes the action regression loss and α controls the strength of the auxiliary regularization.

From an optimization perspective, this objective encourages agreement between the router’s soft probability mass and its hard top- k allocation statistics while disincentivizing concentration on a small subset of experts. Under balanced routing, one expects both $f_i^{(l)}$ and $P_i^{(l)}$ to approach a near-uniform distribution across experts, in which case the loss is minimized up to the top- k sparsity constraint. Consequently, the regularizer improves training stability, prevents persistent expert under-utilization, and promotes more effective specialization across the expert pool. Empirically, this effect is important for maintaining the intended division of labor among specialized experts and for fully exploiting the parameter efficiency of the GSE design.

NeurIPS Paper Checklist

1. Claims

Question: Do the main claims made in the abstract and introduction accurately reflect the paper’s contributions and scope?

Answer: [Yes]

Justification: The abstract and introduction clearly state the motivation, the generalized–specialized expert design, the main methodological components, and the empirical gains of VLA-GSE. These claims are supported by the method, simulation experiments, and real-world experiments presented in the paper.

Guidelines:

- The answer [N/A] means that the abstract and introduction do not include the claims made in the paper.
- The abstract and/or introduction should clearly state the claims made, including the contributions made in the paper and important assumptions and limitations. A [No] or [N/A] answer to this question will not be perceived well by the reviewers.
- The claims made should match theoretical and experimental results, and reflect how much the results can be expected to generalize to other settings.
- It is fine to include aspirational goals as motivation as long as it is clear that these goals are not attained by the paper.

2. Limitations

Question: Does the paper discuss the limitations of the work performed by the authors?

Answer: [Yes]

Justification: The paper now includes a dedicated *Limitations and Future Works* subsection in the Appendix.

Guidelines:

- The answer [N/A] means that the paper has no limitation while the answer [No] means that the paper has limitations, but those are not discussed in the paper.
- The authors are encouraged to create a separate “Limitations” section in their paper.
- The paper should point out any strong assumptions and how robust the results are to violations of these assumptions (e.g., independence assumptions, noiseless settings, model well-specification, asymptotic approximations only holding locally). The authors should reflect on how these assumptions might be violated in practice and what the implications would be.
- The authors should reflect on the scope of the claims made, e.g., if the approach was only tested on a few datasets or with a few runs. In general, empirical results often depend on implicit assumptions, which should be articulated.
- The authors should reflect on the factors that influence the performance of the approach. For example, a facial recognition algorithm may perform poorly when image resolution is low or images are taken in low lighting. Or a speech-to-text system might not be used reliably to provide closed captions for online lectures because it fails to handle technical jargon.
- The authors should discuss the computational efficiency of the proposed algorithms and how they scale with dataset size.
- If applicable, the authors should discuss possible limitations of their approach to address problems of privacy and fairness.
- While the authors might fear that complete honesty about limitations might be used by reviewers as grounds for rejection, a worse outcome might be that reviewers discover limitations that aren’t acknowledged in the paper. The authors should use their best judgment and recognize that individual actions in favor of transparency play an important role in developing norms that preserve the integrity of the community. Reviewers will be specifically instructed to not penalize honesty concerning limitations.

3. Theory assumptions and proofs

Question: For each theoretical result, does the paper provide the full set of assumptions and a complete (and correct) proof?

Answer: [Yes]

Justification: The paper states the assumptions for Theorem 1 in the theorem statement and surrounding text, and provides a full proof in the technical appendix. The theorem, assumptions, and appendix proof are all numbered and cross-referenced.

Guidelines:

- The answer [N/A] means that the paper does not include theoretical results.
- All the theorems, formulas, and proofs in the paper should be numbered and cross-referenced.
- All assumptions should be clearly stated or referenced in the statement of any theorems.
- The proofs can either appear in the main paper or the supplemental material, but if they appear in the supplemental material, the authors are encouraged to provide a short proof sketch to provide intuition.
- Inversely, any informal proof provided in the core of the paper should be complemented by formal proofs provided in appendix or supplemental material.
- Theorems and Lemmas that the proof relies upon should be properly referenced.

4. Experimental result reproducibility

Question: Does the paper fully disclose all the information needed to reproduce the main experimental results of the paper to the extent that it affects the main claims and/or conclusions of the paper (regardless of whether the code and data are provided or not)?

Answer: [Yes]

Justification: The paper discloses substantial information about the model architecture, datasets, parameter counts, training steps, batch size, learning rates, and evaluation protocols.

Guidelines:

- The answer [N/A] means that the paper does not include experiments.
- If the paper includes experiments, a [No] answer to this question will not be perceived well by the reviewers: Making the paper reproducible is important, regardless of whether the code and data are provided or not.
- If the contribution is a dataset and/or model, the authors should describe the steps taken to make their results reproducible or verifiable.
- Depending on the contribution, reproducibility can be accomplished in various ways. For example, if the contribution is a novel architecture, describing the architecture fully might suffice, or if the contribution is a specific model and empirical evaluation, it may be necessary to either make it possible for others to replicate the model with the same dataset, or provide access to the model. In general, releasing code and data is often one good way to accomplish this, but reproducibility can also be provided via detailed instructions for how to replicate the results, access to a hosted model (e.g., in the case of a large language model), releasing of a model checkpoint, or other means that are appropriate to the research performed.
- While NeurIPS does not require releasing code, the conference does require all submissions to provide some reasonable avenue for reproducibility, which may depend on the nature of the contribution. For example
 - (a) If the contribution is primarily a new algorithm, the paper should make it clear how to reproduce that algorithm.
 - (b) If the contribution is primarily a new model architecture, the paper should describe the architecture clearly and fully.
 - (c) If the contribution is a new model (e.g., a large language model), then there should either be a way to access this model for reproducing the results or a way to reproduce the model (e.g., with an open-source dataset or instructions for how to construct the dataset).
 - (d) We recognize that reproducibility may be tricky in some cases, in which case authors are welcome to describe the particular way they provide for reproducibility. In the case of closed-source models, it may be that access to the model is limited in

some way (e.g., to registered users), but it should be possible for other researchers to have some path to reproducing or verifying the results.

5. Open access to data and code

Question: Does the paper provide open access to the data and code, with sufficient instructions to faithfully reproduce the main experimental results, as described in supplemental material?

Answer: [Yes]

Justification: The current submission provides an anonymized code repository.

Guidelines:

- The answer [N/A] means that paper does not include experiments requiring code.
- Please see the NeurIPS code and data submission guidelines (<https://neurips.cc/public/guides/CodeSubmissionPolicy>) for more details.
- While we encourage the release of code and data, we understand that this might not be possible, so [No] is an acceptable answer. Papers cannot be rejected simply for not including code, unless this is central to the contribution (e.g., for a new open-source benchmark).
- The instructions should contain the exact command and environment needed to run to reproduce the results. See the NeurIPS code and data submission guidelines (<https://neurips.cc/public/guides/CodeSubmissionPolicy>) for more details.
- The authors should provide instructions on data access and preparation, including how to access the raw data, preprocessed data, intermediate data, and generated data, etc.
- The authors should provide scripts to reproduce all experimental results for the new proposed method and baselines. If only a subset of experiments are reproducible, they should state which ones are omitted from the script and why.
- At submission time, to preserve anonymity, the authors should release anonymized versions (if applicable).
- Providing as much information as possible in supplemental material (appended to the paper) is recommended, but including URLs to data and code is permitted.

6. Experimental setting/details

Question: Does the paper specify all the training and test details (e.g., data splits, hyperparameters, how they were chosen, type of optimizer) necessary to understand the results?

Answer: [Yes]

Justification: The paper reports many core settings, including the backbone, expert configuration, training steps, batch sizes, learning rates, and evaluation protocols in the Experiments section.

Guidelines:

- The answer [N/A] means that the paper does not include experiments.
- The experimental setting should be presented in the core of the paper to a level of detail that is necessary to appreciate the results and make sense of them.
- The full details can be provided either with the code, in appendix, or as supplemental material.

7. Experiment statistical significance

Question: Does the paper report error bars suitably and correctly defined or other appropriate information about the statistical significance of the experiments?

Answer: [Yes]

Justification: The appendix reports error bars for inference latency.

Guidelines:

- The answer [N/A] means that the paper does not include experiments.
- The authors should answer [Yes] if the results are accompanied by error bars, confidence intervals, or statistical significance tests, at least for the experiments that support the main claims of the paper.

- The factors of variability that the error bars are capturing should be clearly stated (for example, train/test split, initialization, random drawing of some parameter, or overall run with given experimental conditions).
- The method for calculating the error bars should be explained (closed form formula, call to a library function, bootstrap, etc.)
- The assumptions made should be given (e.g., Normally distributed errors).
- It should be clear whether the error bar is the standard deviation or the standard error of the mean.
- It is OK to report 1-sigma error bars, but one should state it. The authors should preferably report a 2-sigma error bar than state that they have a 96% CI, if the hypothesis of Normality of errors is not verified.
- For asymmetric distributions, the authors should be careful not to show in tables or figures symmetric error bars that would yield results that are out of range (e.g., negative error rates).
- If error bars are reported in tables or plots, the authors should explain in the text how they were calculated and reference the corresponding figures or tables in the text.

8. Experiments compute resources

Question: For each experiment, does the paper provide sufficient information on the computer resources (type of compute workers, memory, time of execution) needed to reproduce the experiments?

Answer: [Yes]

Justification: The paper states that training uses 8 NVIDIA A100 GPUs and reports real-world inference latency on an NVIDIA RTX 5080 GPU.

Guidelines:

- The answer [N/A] means that the paper does not include experiments.
- The paper should indicate the type of compute workers CPU or GPU, internal cluster, or cloud provider, including relevant memory and storage.
- The paper should provide the amount of compute required for each of the individual experimental runs as well as estimate the total compute.
- The paper should disclose whether the full research project required more compute than the experiments reported in the paper (e.g., preliminary or failed experiments that didn't make it into the paper).

9. Code of ethics

Question: Does the research conducted in the paper conform, in every respect, with the NeurIPS Code of Ethics <https://neurips.cc/public/EthicsGuidelines>?

Answer: [Yes]

Justification: To the best of our knowledge, the research conforms to the NeurIPS Code of Ethics. The work uses standard simulation benchmarks and robot-policy evaluation, and the paper does not describe practices that would conflict with the code.

Guidelines:

- The answer [N/A] means that the authors have not reviewed the NeurIPS Code of Ethics.
- If the authors answer [No], they should explain the special circumstances that require a deviation from the Code of Ethics.
- The authors should make sure to preserve anonymity (e.g., if there is a special consideration due to laws or regulations in their jurisdiction).

10. Broader impacts

Question: Does the paper discuss both potential positive societal impacts and negative societal impacts of the work performed?

Answer: [Yes]

Justification: The paper includes a dedicated *Impact Statement* subsection in the appendix.

Guidelines:

- The answer [N/A] means that there is no societal impact of the work performed.
- If the authors answer [N/A] or [No], they should explain why their work has no societal impact or why the paper does not address societal impact.
- Examples of negative societal impacts include potential malicious or unintended uses (e.g., disinformation, generating fake profiles, surveillance), fairness considerations (e.g., deployment of technologies that could make decisions that unfairly impact specific groups), privacy considerations, and security considerations.
- The conference expects that many papers will be foundational research and not tied to particular applications, let alone deployments. However, if there is a direct path to any negative applications, the authors should point it out. For example, it is legitimate to point out that an improvement in the quality of generative models could be used to generate Deepfakes for disinformation. On the other hand, it is not needed to point out that a generic algorithm for optimizing neural networks could enable people to train models that generate Deepfakes faster.
- The authors should consider possible harms that could arise when the technology is being used as intended and functioning correctly, harms that could arise when the technology is being used as intended but gives incorrect results, and harms following from (intentional or unintentional) misuse of the technology.
- If there are negative societal impacts, the authors could also discuss possible mitigation strategies (e.g., gated release of models, providing defenses in addition to attacks, mechanisms for monitoring misuse, mechanisms to monitor how a system learns from feedback over time, improving the efficiency and accessibility of ML).

11. Safeguards

Question: Does the paper describe safeguards that have been put in place for responsible release of data or models that have a high risk for misuse (e.g., pre-trained language models, image generators, or scraped datasets)?

Answer: [N/A]

Justification: The paper poses no such risks. Accordingly, this question is not applicable to the current submission.

Guidelines:

- The answer [N/A] means that the paper poses no such risks.
- Released models that have a high risk for misuse or dual-use should be released with necessary safeguards to allow for controlled use of the model, for example by requiring that users adhere to usage guidelines or restrictions to access the model or implementing safety filters.
- Datasets that have been scraped from the Internet could pose safety risks. The authors should describe how they avoided releasing unsafe images.
- We recognize that providing effective safeguards is challenging, and many papers do not require this, but we encourage authors to take this into account and make a best faith effort.

12. Licenses for existing assets

Question: Are the creators or original owners of assets (e.g., code, data, models), used in the paper, properly credited and are the license and terms of use explicitly mentioned and properly respected?

Answer: [Yes]

Justification: The paper credits the sources of existing datasets, baselines, and backbone models through citations in the Experiments Section.

Guidelines:

- The answer [N/A] means that the paper does not use existing assets.
- The authors should cite the original paper that produced the code package or dataset.
- The authors should state which version of the asset is used and, if possible, include a URL.

- The name of the license (e.g., CC-BY 4.0) should be included for each asset.
- For scraped data from a particular source (e.g., website), the copyright and terms of service of that source should be provided.
- If assets are released, the license, copyright information, and terms of use in the package should be provided. For popular datasets, paperswithcode.com/datasets has curated licenses for some datasets. Their licensing guide can help determine the license of a dataset.
- For existing datasets that are re-packaged, both the original license and the license of the derived asset (if it has changed) should be provided.
- If this information is not available online, the authors are encouraged to reach out to the asset's creators.

13. **New assets**

Question: Are new assets introduced in the paper well documented and is the documentation provided alongside the assets?

Answer: [Yes]

Justification: The current manuscript states that new codes are released as assets.

Guidelines:

- The answer [N/A] means that the paper does not release new assets.
- Researchers should communicate the details of the dataset/code/model as part of their submissions via structured templates. This includes details about training, license, limitations, etc.
- The paper should discuss whether and how consent was obtained from people whose asset is used.
- At submission time, remember to anonymize your assets (if applicable). You can either create an anonymized URL or include an anonymized zip file.

14. **Crowdsourcing and research with human subjects**

Question: For crowdsourcing experiments and research with human subjects, does the paper include the full text of instructions given to participants and screenshots, if applicable, as well as details about compensation (if any)?

Answer: [N/A]

Justification: The paper does not involve crowdsourcing or human-subject studies; the real-world experiments are robotic evaluations rather than studies on human participants. Therefore, this question is not applicable.

Guidelines:

- The answer [N/A] means that the paper does not involve crowdsourcing nor research with human subjects.
- Including this information in the supplemental material is fine, but if the main contribution of the paper involves human subjects, then as much detail as possible should be included in the main paper.
- According to the NeurIPS Code of Ethics, workers involved in data collection, curation, or other labor should be paid at least the minimum wage in the country of the data collector.

15. **Institutional review board (IRB) approvals or equivalent for research with human subjects**

Question: Does the paper describe potential risks incurred by study participants, whether such risks were disclosed to the subjects, and whether Institutional Review Board (IRB) approvals (or an equivalent approval/review based on the requirements of your country or institution) were obtained?

Answer: [N/A]

Justification: The paper does not involve crowdsourcing or human-subject research, so IRB review is not applicable to this work.

Guidelines:

- The answer [N/A] means that the paper does not involve crowdsourcing nor research with human subjects.
- Depending on the country in which research is conducted, IRB approval (or equivalent) may be required for any human subjects research. If you obtained IRB approval, you should clearly state this in the paper.
- We recognize that the procedures for this may vary significantly between institutions and locations, and we expect authors to adhere to the NeurIPS Code of Ethics and the guidelines for their institution.
- For initial submissions, do not include any information that would break anonymity (if applicable), such as the institution conducting the review.

16. Declaration of LLM usage

Question: Does the paper describe the usage of LLMs if it is an important, original, or non-standard component of the core methods in this research? Note that if the LLM is used only for writing, editing, or formatting purposes and does *not* impact the core methodology, scientific rigor, or originality of the research, declaration is not required.

Answer: [Yes]

Justification: We have a Statement for Use of LLMs Section to elaborate this. LLMs were only used to assist with language polishing in certain sections of this paper.

Guidelines:

- The answer [N/A] means that the core method development in this research does not involve LLMs as any important, original, or non-standard components.
- Please refer to our LLM policy in the NeurIPS handbook for what should or should not be described.